INVESTIGATION OF THERMAL CHARACTERISTICS OF A SERIES POLYOXAZOLINES BY DIRECT PYROLYSIS MASS SPECTROMETRY

A THESIS SUBMITTED TO
THE GRADUATE SCHOOL OF NATURAL AND APPLIED SCIENCES
OF
MIDDLE EAST TECHNICAL UNIVERSITY

BY

NURCAN ATILKAN

IN PARTIAL FULFILLMENT OF THE REQUIREMENTS
FOR
THE DEGREE OF MASTER SCIENCE
IN
POLYMER SCIENCE AND TECHNOLOGY

FEBRUARY 2011

Approval of thesis:

INVESTIGATION OF THERMAL CHARACTERISTICS OF A SERIES POLYOXAZOLINES BY DIRECT PYROLYSIS MASS SPECTROMETRY

submitted by **NURCAN ATILKAN** in partial fulfillment of the requirements for the degree of **Master of Science in Polymer Science and Technology Department, Middle East Technical University** by,

Prof. Dr. Canan Özgen _____
Dean, Graduate School of **Natural and Applied Sciences**

Prof. Dr. Necati Özkan _____
Head of Department, **Polymer Science and Technology**

Prof. Dr. Jale Hacaloğlu _____
Supervisor, **Chemistry Department, METU**

Prof. Dr. Levent Toppare _____
Co-Supervisor, **Chemistry Department, METU**

Examining Committee Members

Prof. Dr. Ahmet M. Önal _____
Chemistry Dept., METU

Prof. Dr. Jale Hacaloğlu _____
Chemistry Dept., METU

Prof. Dr. Levent Toppare _____
Chemistry Dept., METU

Prof. Dr. Göknur Bayram _____
Chemical Engineering Dept., METU

Assoc. Prof. Dr. Yasemin Arslan Udum _____
Advanced Technologies Dept., Gazi University

Date:09/02/2011

I hereby declare that all information in this document has been obtained and presented in accordance with academic rules and ethical conduct. I also declare that, as required by these rules and conduct, I have fully cited and referenced all material and results that are not original to this work.

Name, Last name: Nurcan Atılkan

Signature:

ABSTRACT

INVESTIGATION OF THERMAL CHARACTERISTICS OF A SERIES POLYOXAZOLINES BY DIRECT PYROLYSIS MASS SPECTROMETRY

Atılkan, Nurcan

M.Sc., Department of Polymer Science and Technology
Supervisor: Prof. Dr. Jale Hacaloğlu
Co-Supervisor: Prof. Dr. Levent Toppare

February 2011, 69 pages

In the latest years, many studies especially on characterization and synthesis of polyoxazolines have been made. During these studies, new polyoxazolines such as poly(2-isopropyl-2-oxazoline) (PIPOX), poly(2-(3-butenyl)-2-oxazoline) (PBOX) and modified PBOX were synthesized. However, there has been no investigation on their thermal characteristics such as thermal stability and thermal degradation products.

In this study, thermal degradation characteristics, thermal degradation products and thermal stability of PIPOX, PBOX and modified PBOX polymers PBOX-Perf, PBOX-Thiop, PBOX-Sug, PBOX-SP and PBOX-TP were investigated. In this study mercaptans 1H,1H,2H,2H-perfluoro-octanethiol, 3-mercapto-1,2 propanediol, thio-β-D-glucose derivative and their mixture were used in PBOX modifications. The effect of modification of PBOX with different mercaptans on thermal characteristics was also analyzed.

For the PIPOX, formations of protonated monomer and oligomers from dimer to heptamer were observed. However, when the isopropyl group changes with 3-butenyl group, protonated oligomers up to trimer were observed because the crosslinking formed during the polymerization of unsaturated butenyl inhibited the production of oligomers. In addition to this, thermal degradation at lower temperatures was observed.

The change in thermal stability and thermal degradation products were observed as a result of modification of PBOX with different mercaptans. Unlike PBOX-Sug thermal degradation started at very low temperatures for PBOX-Thiop and PBOX-Perf. This degradation observed at lower temperatures disappeared for PBOX-SP and PBOX-TP. For PBOX-Perf, PBOX-Sug and PBOX- Thiop, decomposition of side chains at low temperatures and decomposition of the main chain at high temperatures were observed.

Although the same thermal degradation behavior for PBOX-TP and PBOX-Thiop was expected, since PBOX-TP was obtained as a result of modification of PBOX with high amounts of mercaptan used in PBOX-Thiop and small amounts of mercaptan used in the PBOX-Perf, the results show that neither PBOX-Thiop nor PBOX-Perf thermal degradation behavior are dominant. This is also valid for PBOX-SP. PBOX-SP has higher thermal stability when compared to PBOX-Sug.

Keywords: Poly(2-isopropyl-2-oxazoline) (PIPOX), poly(2-(3-butenyl)-2-oxazoline) (PBOX) , modified PBOX, thermal degradation, direct pyrolysis mass spectrometry.

ÖZ

DİREKT PİROLİZ KÜTLE SPEKTROMETRESİ İLE BİR SERİ POLİOKZASOLİNLERİN ISISAL KARAKTERİSTİĞİNİN İNCELENMESİ

Atılkan, Nurcan

Yüksek Lisans, Polimer Bilim ve Teknolojisi Bölümü
Tez Yöneticisi : Prof. Dr. Jale Hacaloğlu
Ortak Tez Yöneticisi: Prof. Dr. Levent Toppare

Şubat 2011, 69 sayfa

Son yıllarda özellikle poliokzasolinlerin karakterizasyonu ve sentezleri ile ilgili olarak bir çok çalışma yapılmıştır. Bu çalışmalar esnasında poli(2-izopropil-2-okzasolin) (PIPOX), poli(2-(3-bütenil)-2-okzasolin) (PBOX)ve modifiye PBOX gibi yeni poliokzasolinler sentezlenmiştir. Fakat bu poliokzasolinlerin ısısal kararlılık ve ısısal bozunum ürünleri gibi ısısal karakteristikleri ile ilgili inceleme yoktur.

Bu çalışmada PIPOX, PBOX ve modifiye edilmiş PBOX polimerleri PBOX-Perf, PBOX-Thiop, PBOX-Sug, PBOX-SP ve PBOX-TP'nin ısısal bozunum karakteristiği, ısısal bozunum ürünleri ve ısısal kararlılığı incelenmiştir. Bu çalışmada, 1H,1H,2H,2H- perflorooktantiyol, 3-merkapto-1,2 propandiol, thio-β-D-gilikoz türevi ve bunların karışımı merkaptanlar PBOX modifikasyonlarında kullanılmıştır. PBOX'ın farklı merkaptanlar ile modifikasyonunun ısısal karakteristiğe olan etkisi de analiz edilmiştir.

PIPOX için protonlanmış monomer ve dimerden heptamere kadar oligomer oluşumu gözlemlenmiştir. Ancak izopropil grubu 3-bütenil grubu ile değiştiğinde, trimere kadar protanlanmış oligomer oluşumu gözlemlenmiştir. Doymamış bütenilin polimerizasyonu esnasında oluşan çapraz bağlı yapı oligomer oluşumunu engellemiştir. Bunun yanı sıra daha düşük sıcaklıklarda ısısal bozunum gözlenmiştir.

PBOX'ın farklı merkaptanlar ile modifikasyonu sonucunda ısısal kararlılık ve ısısal bozunum ürünlerinde değişiklikler gözlemlenmiştir. PBOX-Thiop ve PBOX-Perf için PBOX-Sug'dan farklı olarak ısısal bozunumlar çok düşük sıcaklıklarda başlamıştır. Düşük sıcaklıklarda gözlenen bu bozunum PBOX-SP ve PBOX-TP için kaybolmuştur. PBOX-Perf, PBOX-Sug and PBOX- Thiop için, düşük sıcaklıklarda yan zincirlerin bozulması ve yüksek sıcaklıklarda ana zincirin bozulması gözlemlenmiştir.

PBOX-TP, PBOX'ın yüksek miktarda PBOX-Thiop'ta kullanılan merkaptan ve çok az miktarda PBOX-Perf'te kullanılan merkaptan ile modifiye edilmesiyle elde edilmiş olmasından dolayı PBOX-TP ve PBOX-Thiop için aynı ısısal bozunum davranışı beklenilmesine rağmen, sonuçlar ne PBOX-Thiop ne de PBOX-Perf'in ısısal bozunum davranışının baskın olmadığını göstermiştir. Bu durum PBOX-SP içinde geçerlidir. PBOX-SP, PBOX-Sug ile kıyaslandığında daha yüksek ısısal kararlılığa sahiptir.

Anahtar kelimeler: Poli(2-izopropil-2-okzasolin) (PIPOX), poli(2-(3-bütenil)-2-okzasolin) (PBOX) ve modifiye edilmiş PBOX, ısısal bozunum, direkt piroliz kütle spektrometresi.

TO MY DEAR FAMILY

ACKNOWLEDGEMENTS

I would like to express my deepest gratitude to my supervisor Prof.Dr. Jale Hacaloğlu for her support and guidance throughout my thesis. Without her advices and endless patience, this thesis wouldn't have been possible to accomplish.

I would also like to thank my co-advisor Prof.Dr. Levent Toppare for his support.

I would also like to express my special thanks to Yusuf Nur for his friendship, technical advices and encouragements.

Finally, I would like to thank to my family for their endless support during my study.

TABLE OF CONTENTS

LIST OF FIGURES

FIGURES

LIST OF TABLES

TABLES

LIST OF SCHEMES

SCHEMES

ABBREVIATIONS

a.m.u.	Atomic mass unit
Da	Dalton
DP-MS	Direct Pyrolysis Mass Spectrometry
LCST	Lower Critical Solution Temperature
M	Monomer
MS	Mass Spectrometry
n	number of repeating units
PBOX	Poly(2-(3-butenyl)-2-oxazoline)
PBOX-Perf	Modified poly(2-(3-butenyl)-2-oxazoline) with 1H,1H,2H,2H-perfluoro-octanethiol
PBOX-Thiop	Modified Poly(2-(3-butenyl)-2-oxazoline) with 3-mercapto-1,2 propanediol
PBOX-Sug	Modified Poly(2-(3-butenyl)-2-oxazoline) with thio-β-D-glucose derivative
PBOX-SP	Modified poly(2-(3-butenyl)-2-oxazoline) with thio-β-D-glucose derivative and 1H,1H,2H,2H-perfluoro-octanethiol
PBOX-TP	Modified poly(2-(3-butenyl)-2-oxazoline) with 3-mercapto-1,2 propanediol and 1H,1H,2H,2H-perfluoro-octanethiol
PIPOX	Poly(2-isopropyl-2-oxazoline)
PNIPAM	Poly(N-isopropyl acrylamide)
Py	Pyrolysis
RI	Relative Intensity

CHAPTER 1

INTRODUCTION

1.1 Stimuli-responsive Polymers

Stimuli-responsive polymers, also called as smart polymers are one of the most important groups of polymers and their applications in many areas have been increasing since their invention [1, 2]. Biotechnology, medicine and engineering are main application areas of smart polymers [1-3]. With the developments of smart polymers in the last decade, they have found new usages. They can be used in the areas such as bioseparations, protein folding, drug delivery, other metabolic control mechanisms, microfluidics and smart surfaces [1].

The physical and chemical properties of these type of polymers change considerably with small changes in their environment [4]. Temperature, light, pH, chemical species, ultra violet radiation, electric and magnetic field can be given as the examples of properties that affect polymers [4-6]. Investigations on the effects of external stimuli were carried out by Heskins and Guillet as early as 1960s [7].

Thermoresponsivity is the most thoroughly exploited smart property of polyoxazolines [3, 8]. Thermoresponsive polymer undergoes large changes in properties when external thermal stimuli are presented [9]. The most thoroughly investigated and a well-known thermoresponsive polymer is poly(N-isopropyl acrylamide) (PNIPAM). Its lower critical solution temperature (LCST) is around 32 ºC and this value is very close to human body temperature [3, 10]. Thermoresponsive polymers become more hydrophobic (less soluble) in water at elevated temperatures. This behavior is not observed for most polymers in aqueous

solutions. Several polyoxazolines show transition from soluble to insoluble near to human body temperature [3, 11]. This property makes them usable in biomedical applications such as drug delivery, tissue engineering and bio functional molecular techniques.

1.2 Poly(2-alkyl-2-oxazoline)s

Although poly(N-isopropyl acrylamide) (PNIPAM) is the most widely known and studied thermoresponsive polymer, the major disadvantage of PNIPAM is that it undergoes strong hysteresis [12]. Poly(2-oxazoline)s could be a better alternative to PNIPAM because they exhibit a reversible, concentration dependent phase separation and do not show hysteresis [12].

The general formula of poly(2-alkyl-2-oxazoline)s an example of stimuli responsive polymers is shown in Scheme 1.1 where R group is $CH(CH_3)_2$, $CH_2CH_2CH{=}CH_2$ and $CH_2CH_2CH_2CH_2S\text{-}R_1$.

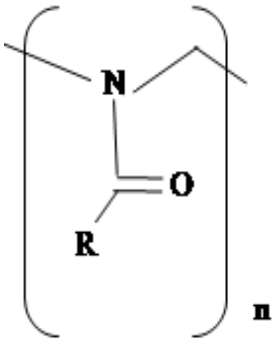

Scheme 1.1: The general formula of poly(2-alkyl-2-oxazoline)s

Poly(2-alkyl-2-oxazoline)s are also called as poly(N-acyl ethylene imine)s or poly(N-acyl aziridine)s [8]. They are regarded as structural isomers of polyamides [3, 13, 14] and also considered as pseudopeptides because of the structural relation to polypeptides [15].

The living cationic ring opening polymerization of poly(2-alkyl-2-oxazoline)s was discovered back in 1966 [16]. However, due to their long reaction times and having not sufficient applications, poly(2-alkyl-2-oxazoline)s was almost forgotten in the 1980s and 1990s [17]. There have been recent developments in polymer technology especially the advent of microwave reactors. Use of microwave reactors in polymer synthesis enabled easy access to operation conditions especially high-temperature/high-pressure conditions [18-20]. Polymerizations can be carried out in short reaction times [18]. As a result, a revival of poly(2-alkyl-2-oxazoline)s has arisen in the new millennium.

One of the important features of poly(2-alkyl-2-oxazoline)s is the ease of preparation of co-polymers [6, 18, 21]. Another important feature of poly(2-alkyl-2-oxazoline)s is the possible ease of introducing functional groups via initiators, monomers and terminating agents. In the past, they have found applications in adhesives, photo resists, inks, coatings, compatibilizing agents in personal care products, modified, regenerated cellulosic [22] but they have recently found interesting new application areas especially in biology and biomedicine [17]. They can be used as biomaterials because they are water soluble and relatively non toxic [13, 23]. In addition amphiphilic poly(2-oxazoline)s have also taken into consideration due to their applications as hydrogels, aqueous self-assembly, micellar catalysis and drug delivery [24].

The studies on synthesis and microwave polymerization of 2-substituted-2-oxazolines have been appeared in literature [19, 25, 26]. New multifunctional copoly(2-oxazoline) nanoparticles for cell studies were also prepared [27].

Poly(2-alkyl-2-oxazoline)s can be synthesized by living/controlled cationic polymerization and polymer ('click') modification procedures [13, 25]. It was possible to obtain water soluble, water insoluble, fluorophilic, hard and soft materials from copolymerization of a variety of 2-oxazoline monomers using living polymerization method.

Studies related with poly(2-alkyl-2-oxazoline)s especially poly(2-isopropyl-2-oxazoline) (PIPOX) are focused on factors affecting lower critical solution temperature (LCST) [1, 3, 5, 6, 8, 10, 12-14, 18, 21, 24, 25, 28, 29] because LCST is an important parameter in the determination of polymer usages in biological applications. LCST is the temperature at which a polymer becomes insoluble in water and precipitates [21]. LCST can be increased or decreased respectively by introducing hydrophilic or hydrophobic moieties, according to the requirements of the applications [14]. Polymers carrying short alkyl side groups (methyl, ethyl, propyl and isopropyl) are hydrophilic [8]. Polymers displaying LCST are soluble below their LCST due to hydrogen bonds that are formed with the solvent. As a result of these bonds, hydration shell around the polymer forms [11]. Above LCST, the polymer becomes hydrophobic and precipitates. Polymeric matrix is used as enclosure for drugs. It is aimed to release of the active agent in drug over time through diffusion [18]. When the drug is enclosed in polymer, compared to pure drug molecule it has the following advantages; a) reduction of the transport of bioactive molecules out of the hydrogels by means of formation of thick skin surface above the LCST [30], b) increase in the solubility of insoluble drugs or low aqueous soluble drugs, c) prevention of drug from deactivation and degradation during transport and circulation [18].

Poly(2-alkyl-2-oxazoline)s' properties such as crystallinity or solubility depends on the nature of side chain R [13]. Among the various poly(2-alkyl-2-oxazoline)s, only those possessing short alkyl groups are soluble in water below the LCST [23].

There has been no study on the thermal degradation mechanism of poly(2-alkyl-2 oxazoline)s. The thermal degradation mechanism of poly(2-alkyl-2oxazoline)s is important in the determination of the application areas.

1.2.1 Poly(2-isopropyl-2-oxazoline) (PIPOX)

When 2-substituted-2-oxazolines are polymerized, the properties of the resulting polymer depend on the substituent group. The potential synthesis of substituted 2-oxazolines makes the preparation of new functional polymers possible [31]. In addition this enables the base data required for the future design of new polymers with estimated properties [31].

Poly(2-isopropyl-2-oxazoline) **(**PIPOX) was introduced by Kobayashi and Uyama and Kataoka et.al. Thermoresponsivity and crystallinity of PIPOX are its advantageous properties [8]. LCST of PIPOX varies in the narrow range of 38.5 °C (n=47) and 35.5 °C (n=147) [3]. PIPOX has attracted much attention among poly(2-alkyl-2-oxazoline)s because it can be used in biomedical applications due to its LCST, very near to human body temperature [23].

Researches on PIPOX are mainly based on the synthesis and characterization of the synthesis [10, 14, 19, 29, 31-34], demixing and remixing kinetics [28], the kinetics of the crystallization [2, 3, 9], formation of nanomaterials [8, 23], copolymerization [6, 10, 12, 29] and mechanical properties [35]. In this scope, scanning force microscopy (SFM), differential scanning calorimetry (DSC), x-ray diffraction (XRD), cryogenic scanning electron microscopy (Cryo-SEM), scanning electron microscopy (SEM) and transmission electron microscopy (TEM) were used in analyses [3, 9, 13, 36]. Schubert and coworkers used gas chromatography-mass spectrometry (GC-MS) to characterize synthesized 2-oxazolines [30]. Matrix-assisted laser desorption/ionization-time of flight (MALDI-TOF) mass spectrometry was used to find the respective monomer reactivity ratios [6].

1.2.2 Poly(2-(3-butenyl)-2-oxazoline) (PBOX) and Modified PBOX

The living/controlled cationic polymerization of 2-(3-butenyl)-2-oxazoline to give PBOX was firstly achieved in 2007 by Schlaad and coworkers [37]. The radical addition of mercaptans (RSH) onto PBOX was also achieved in 2007 [37].

PBOX was modified with several mercaptans, namely 1H,1H,2H,2H-perfluoro-octanethiol (PBOX-Perf) , thio-β-D-glucose derivative (PBOX-Sug) and 3-mercapto-1,2 propanediol (PBOX-Thiop) by Schlaad and coworkers recently [13, 37, 38, 39].

PBOX was modified with a mixture of 99% thio-β-D-glucose derivative and 1% 1H,1H,2H,2H-perfluoro-octanethiol to obtain PBOX-SP1 and with a mixture of 99% 3-mercapto-1,2 propanediol and 1% 1H,1H,2H,2H-perfluoro-octanethiol to obtain PBOX-TP1.

Thio-β-D-glucose derivative and 3-mercapto-1,2 propanediol have hydroxyl groups. Thermoresponsive property can be expected when polyoxazolines carry hydroxyl groups in the side chains [12]. Fluoropolymers are hydrophobic [37]. 1H,1H,2H,2H-perfluoro-octanethiol and 3-mercapto-1,2 propanediol were also used as mercaptans in the preparation of modified amphiphilic 1,2-polybutadiene block poly(ethylene oxide)s [38]. By free radical addition of thio-β-D-glucose derivative onto polybutadiene base, formation of diblock copolymers was studied in 2006 [39]. Nanofibers of modified PBOX with thio-β-D-glucose derivative were obtained by formation of hydrogen bonding [9].

The characterization of PBOX and modified PBOX were done by means of NMR spectroscopy, fourier-transform infrared spectroscopy (FT-IR), analytical ultracentrifugation (AUC) and size exclusion chromatography (SEC) techniques [37].

The properties of PBOX and modified PBOX have been under investigation.

1.3 Thermal Degradation

Thermal degradation is molecular deterioration of a polymer due to exposure to excessive heat. When a polymer is exposed to excess heat, the components of the polymer can begin to break down. As a result of thermal degradation, the polymer molecular weight changes. As a result of this change, physical and mechanical properties such stiffness, strength, viscoelasticity, toughness and viscosity will not be the same with the initially specified properties.

Several techniques can be used for the determination of thermal degradation of polymers. In thermogravimetric analysis (TGA) technique, change in the amount of sample as a function of temperature is determined. Differential scanning calorimetry (DSC) is another technique. In this technique, the difference in the amount of heat required to increase the temperature of sample and a reference as a function of temperature is measured. Differential thermal analysis (DTA) is another technique. Both the material and an inert reference undergo identical thermal cycles, while recording the temperature difference between sample and reference.

1.4 Pyrolysis

Pyrolysis is the thermal degradation of a complex material in an inert atmosphere or in the absence of oxygen. The most common application area of pyrolysis is investigation of thermal properties of a compound, which can be summarized as thermal stability, products generated as a result of degradation and decomposition mechanism. To prevent oxidation reactions, pyrolysis is done under vacuum in other words under oxygen-free atmosphere. However, it is not possible to completely remove air from the system.

Thermal stability depends on the relative strength of the bonds which hold the molecule together. As a result of heating, the thermal energy may be distributed about all modes of excitation and when the vibrational excitation is greater than the energy of specific bonds, the decomposition of molecule occurs. Thermal

decomposition of a compound at any specific temperature always occurs in a reproducible way producing fingerprint. Pyrolysis temperature and heating rate are two important factors to be strictly controlled to ensure the reproducibility. Pyrolysis technique can be coupled with FT-IR, GC (Py-GC), GC/MS (Py-GC/MS) or MS (DP-MS). Among these various analytical pyrolysis techniques, pyrolysis gas chromatography mass spectrometry, Py-GC/MS or direct pyrolysis mass spectrometry, DP-MS, have several advantages such as sensitivity, reproducibility, minimal sample preparation and consumption and speed of analysis .

Mass spectrometry (MS) has gained prominence in the field of polymer synthesis and the characterization of macromolecules, particularly since the advent of the so-called soft-ionization protocols, including electrospray ionization (ESI) and matrix assisted laser desorption/ionization (MALDI) [40].

1.5 Py GC-Mass Spectrometry

There are two components in Py GC-Mass Spectrometry. One is gas chromatography (GC) and the other is the mass spectrometer (MS). In the first, the chemical mixture is separated into pulses of pure chemicals and in the second the chemicals are identified and quantified.

The pyrolysis of the sample performed in a selected pyrolyzer generates a mixture of chemicals. The components of the mixture separated by GC based on their volatilities are identified by MS.

Interpretation of the data obtained from Py GC-Mass Spectrometry is relatively simple. However, with this technique as the products are separated in GC before the analysis by MS, secondary reactions cannot be eliminated. Unstable thermal degradation products cannot be detected.

1.6 Direct Pyrolysis-Mass Spectrometry

The concept of combining a pyrolysis inlet system with a mass spectrometer (MS) has been utilized to provide fingerprint analysis and to study thermal degradation of materials. Pyrolysis-MS (Py-MS) has found applications in a wide range of analytical fields, including the study of synthetic polymers, biochemistry, geochemistry and environmental studies.

Contrary to Py GC-Mass Spectrometry, very complex data is obtained. However, it is possible to eliminate secondary reactions. In addition, both stable and unstable thermal degradation products can be detected.

DP-MS technique has several advantages such as minimal sample preparation and consumption, ability to analyze complex mixtures, selectivity for organic constituents and high reproducibility.

1.7 Mass Spectrometry

The principle of the mass spectrometry is the generation of ions and separation of them according to their mass to charge ratio (m/z). It can be used both qualitative and quantitative purposes. Unknown compounds can be identified and also isotopic composition of elements in a molecule can be determined by means of mass spectrometry. The structure of a compound can also be determined by observing its fragmentation. Another application of MS is determination of the amount of a compound in a sample.

The principle components of mass spectrometer are shown in Figure 1.1. Firstly, sample is introduced onto the MS instrument where sample is vaporized. The components of volatilized sample are ionized by using ion source such as electron impact. As a result of ionization, charged particles (ions) form. Ions are separated in mass analyzer according to their mass to charge ratio. This separation is done by applying electromagnetic fields. As a result, ions formed during analysis are detected.

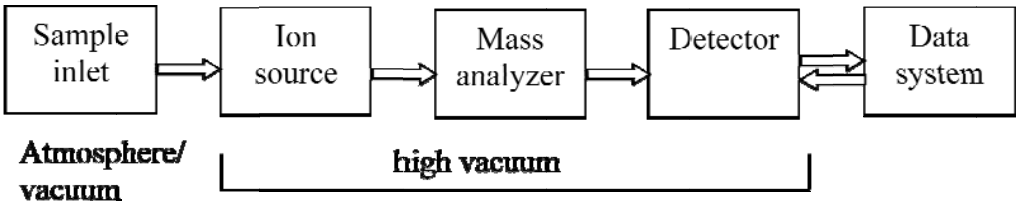

Figure 1.1: General scheme of mass spectrometer.

1.7.1 The Ion Source

Micromole or even less sample is volatilized and allowed to leak slowly into the ionization area. The sample under analysis is ionized in the ion source part of the mass spectrometer. The ions are then transported to the mass analyzer by magnetic or electric fields.

There are many ionization techniques such as electron impact ionization (EI), chemical ionization (CI), electrospray ionization (ES), laser ionization (LI), thermal ionization (TI), field ionization (FI), matrix-assisted laser desorption ionization (MALDI), plasma-desorption ionization (PD), resonance ionization (RI), fast-atom bombardment (FAB). According to the type of the sample, ionization technique is chosen. Chemical and electron ionization techniques are suitable for samples in the form of gas and vapor. For liquid and solid samples, matrix-assisted laser desorption and electrospray ionization are often used.

Electron ionization is the most widely used technique in mass spectrometry. It is used for the analysis of low to medium polarity, nonionic or organic compounds having the molecular weights up to 1000.

Electrons are produced by heating a wire filament. The electrons are accelerated to 70 eV. This acceleration occurs in the region between the filament and the entrance

to the ion source block. The accelerated electrons are then concentrated into a beam by being attracted to the trap electrode. There will be collision between sample and electrons. During this collision, the sample is ionized and both negatively and positively charged ions are produced. Most of the analytical methods are based upon positively charged ions because the number of positively charged ions is always greater than negatively charged ions. The chemistry of the analyte and the energy of the electrons are two main factors affecting the ionization efficiency and production of fragment ions.

1.7.2 The Mass Analyzer

The separation of the ions according to their mass to charge ratio is done by means of mass analyzers. All mass analyzers use either static or dynamic fields, and electric or magnetic fields that can be used alone or combined. Time-of-flight, quadrupole mass filter, three-dimensional quadrupole ion trap, fourier transform ion cyclotron resonance are some types of mass analyzers.

In the quadrupole mass filter analyzer, there are four parallel electric poles. Ions travel with constant velocity in the direction parallel to the poles. Electrically and radio frequency voltage is applied between the poles. As a result of this, ions acquire oscillation. Ions of only a single m/z value will reach the detector for a given ratio of voltages. All other ions having unstable oscillations will strike poles.

1.7.3 Detector

The final part of the mass spectrometer is the detector. Ion-to-photon detectors, electron multiplier and Faraday cups can be used as detectors. The charge induced or the current produced is recorded by means of detector. Ion intensity versus mass to charge ratio graph is obtained as a mass spectrum.

1.8 Aim of the work

In this study, the thermal degradation characteristics, thermal stability, thermal degradation products and thermal decomposition mechanisms of polyoxazolines poly(2-isopropyl-2-oxazoline) (PIPOX), poly(2-(3-butenyl)-2-oxazoline) (PBOX) and their modified analogues PBOX polymers PBOX-Perf, PBOX-Thiop, PBOX-Sug, PBOX-SP and PBOX-TP obtained with the use of mercaptans 1H,1H,2H,2H-perfluoro-octanethiol, 3-mercapto-1,2 propanediol, thio-β-D-glucose derivative and their mixture were analyzed. The effect of modification of PBOX with different mercaptans on thermal characteristics was also investigated.

CHAPTER 2

EXPERIMENTAL

2.1 Materials

Polymers used in this study were synthesized by Helmut Schlaad and coworkers. These polymers were obtained by cationic ring-opening polymerization and thio click modification [13, 14, 37].

In general, anhydrous conditions are required for the cationic ring-opening polymerization of 2-substituted-2-oxazolines. Initiators for the polymerization of oxazolines can be Lewis acids, strong protic acids and their esters, benzyl and alkyl halides and oxazolinium salts. To quench polymerization, nucleophile such as water, alcohol or amine is used. Polymerization duration can be reduced from several days to several minutes by using microwave reactors [5, 13, 14].

2.1.1 Poly (2-isopropyl-2-oxazoline) (PIPOX)

Chemical structure of PIPOX is given in Scheme 2.1.

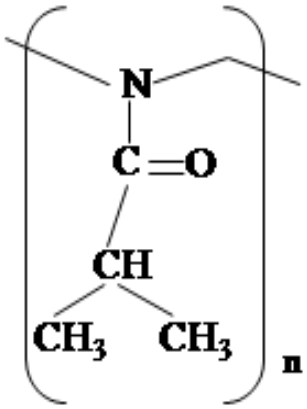

Scheme 2.1: Chemical structure of PIPOX (n is the number of repeating units)

2.1.2 Poly (2-(3-butenyl)-2-oxazoline) (PBOX)

Chemical structure of PBOX is given in Scheme 2.2.

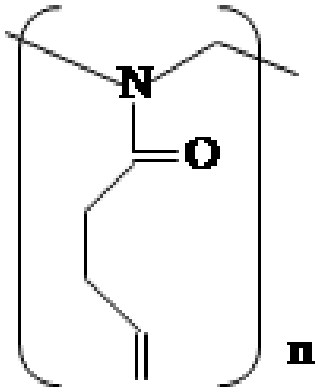

Scheme 2.2: Chemical structure of PBOX

2.1.3 Modified PBOX

Modified polymers were synthesized by Schlaad and coworkers [13, 37]. PBOX was modified as follows. Tetrahydrofuran **(**THF**)** or THF/methanol was used as solvent. Reactants (PBOX and mercaptan) and solvent were placed in glass vessel and exposed to an UV light source for 24 hours. The polymer solution was dialyzed against deionized water.

Thio click modification of PBOX is shown below.

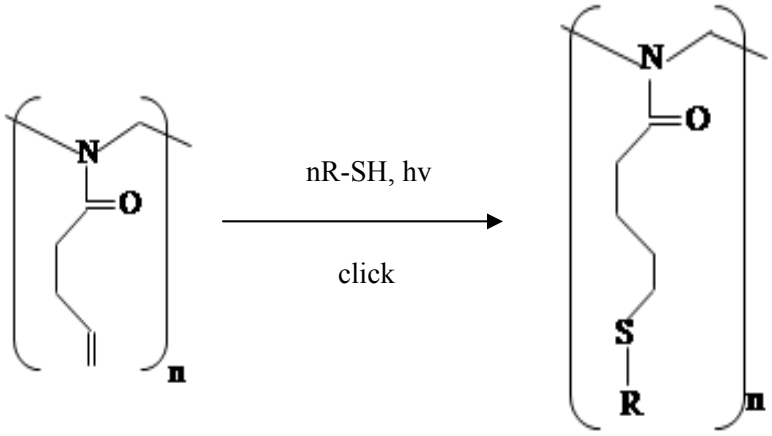

Scheme 2.3: Thio click modification of PBOX

2.1.3.1 PBOX-Perf

PBOX-Perf was obtained by means of modification of PBOX with 1H,1H,2H,2H-perfluoro-octanethiol. Chemical structure of PBOX-Perf is given in Scheme 2.4.

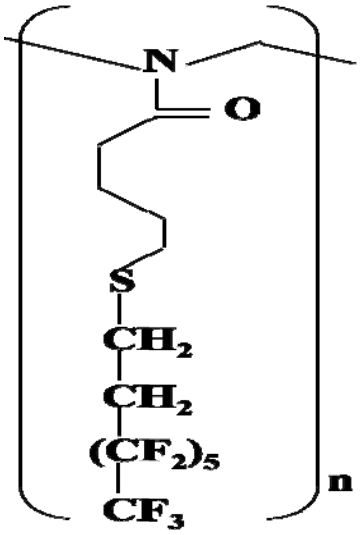

Scheme 2.4: Chemical structure of PBOX-Perf

Chemical structure of mercaptan 1H,1H,2H,2H-perfluoro-octanethiol is given in Scheme 2.5.

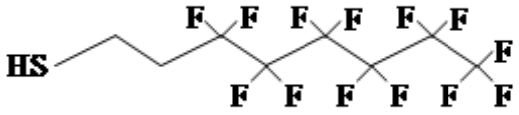

Scheme 2.5: Chemical structure of 1H,1H,2H,2H-perfluoro-octanethiol.

2.1.3.2 PBOX-Sug

As a result of modification of PBOX with Thio-β-D-glucose derivative, PBOX-Sug was obtained. Chemical structure of PBOX-Sug is given in Scheme 2.6. Thio-β-D-glucose derivative was obtained from 2,3,4,6-tetra-O-acetyl-1-thio-β-D-glucopyranose.

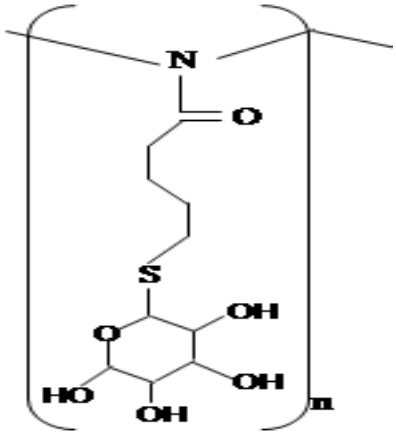

Scheme 2.6: Chemical structure of PBOX-Sug

Chemical structure of 2,3,4,6-tetra-O-acetyl-1-thio-β-D-glucopyranose is given in Scheme 2.7.

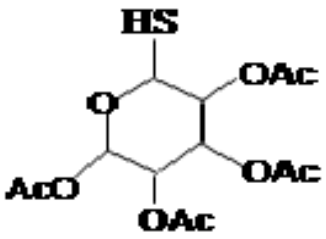

Scheme 2.7: Chemical structure of 2,3,4,6-tetra-O-acetyl-1-thio-β-D-glucopyranose

2.1.3.3 PBOX-Thiop

This polymer was obtained by modification of PBOX with 3-mercapto-1,2 propanediol. Chemical structure of PBOX-Thiop is given in Scheme 2.8.

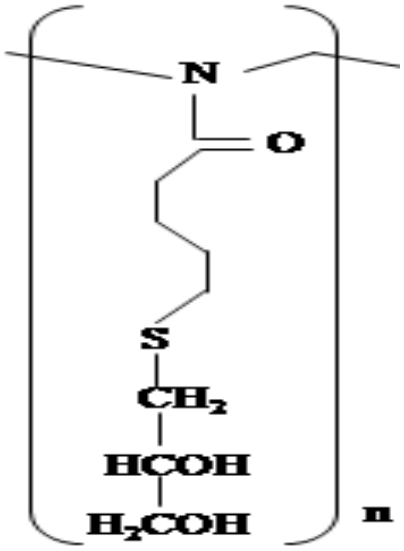

Scheme 2.8: Chemical structure of PBOX-Thiop.

Chemical structure of mercaptan 3-mercapto-1,2 propanediol is given in Scheme 2.9.

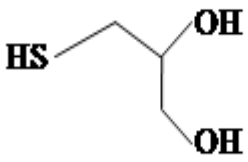

Scheme 2.9: Chemical structure of 3-mercapto-1,2 propanediol.

2.1.3.4 PBOX-SP1

PBOX was modified with a mixture of 99% Thio-β-D-glucose derivative and 1% 1H,1H,2H,2H-perfluoro-octanethiol to obtain PBOX-SP1.

2.1.3.5 PBOX-TP1

PBOX-TP1 was obtained by modifying PBOX with a mixture of 99% 3-mercapto-1,2 propanediol and 1% 1H,1H,2H,2H-perfluoro-octanethiol.

2.2 Mass Spectrometer

Direct pyrolysis Mass Spectrometry method was used in this study. Experiments were performed by using 5973 HP quadrupole mass spectrometry system coupled to a JHP SIS direct insertion probe. During the pyrolysis, mass spectra were recorded at a scan rate of 2 scan/s in the mass range of 10-800 a.m.u.
The major components of the mass spectrometer are vacuum system, sample inlet, ion source, mass filter, detector and the data system (Figure 1.1).

2.2.1 Vacuum System

In the vacuum system, high vacuum (low pressure) required for the mass spectrometer is maintained. Vacuum enables movement of ions generated by electron impacts from the ion source to the quadrupole analyzer and finally to the detector. Vacuum also inhibits collisions of ions with other ions and molecules during this movement. A high vacuum was obtained by diffusion pumps.

2.2.2 Sample Inlet

The Direct Insertion Probe Pyrolysis technique is employed by a SIS direct inlet probe. To control the heating rate, thermocouple attached to the probe tip inside the probe rod is used. There is direct contact between probe tip and flared glass sample vials.

The heating rates are adjusted by using probe software. Ramping heating was applied. For each direct pyrolysis experiments, the following heating programme was used. Initial temperature was 50 °C and the temperature was increased to 445 °C by heating rate of 20 °C/min. The temperature was kept additional 5 minutes at 445 °C.

2.2.3 Ion Source

Sample molecules enter the ion source from the sample inlet. Before the ion source, the sample molecules must be converted into the pyrolyzed form. In the ion source, ionization and fragmentation of the molecules are occurred.

The ion source operates by electron impact ionization (EI). In electron impact ionization, the sample molecules are bombarded with high energy electrons and then positive ions are produced. Since EI produces a large number of fragment ions, it is a hard ionization method and useful for structural information. In this study, in general the ionization energy used was 70 eV.

2.2.4 Mass Analyzer

Separations of ions according to their mass to charge ratio (m/z) are done in the mass filter. At a given radio frequency (RF) to direct current (DC) ratio, only ions of a selected mass to charge ratio can pass through the mass filter to the detector. The analyzer was a quadrupole mass filter and amplifies.

2.2.5 Detector

The detector in the spectrometer is a high energy conversion dynode (HED) coupled to an electron multiplier (EM). The detector is located at the exit end of the quadrupole mass filter. It receives the ions that have passed through the mass filter.

CHAPTER 3

RESULTS AND DISCUSSION

Thermal characteristics including thermal stability and thermal degradation products of poly(2-isopropyl-2-oxazoline) (PIPOX), poly(2-(3-butenyl)-2-oxazoline) (PBOX) and modified PBOX polymers PBOX-Perf, PBOX-Thiop, PBOX-Sug, PBOX-SP and PBOX-TP were investigated via direct pyrolysis mass spectrometry. The effect of modification of PBOX with different mercaptans on thermal degradation was also analyzed.

3.1 Poly(2-isopropyl-2-oxazoline) (PIPOX)

The total ion current (TIC) curve (variation of total ion yield as a function of time and/or temperature) of poly(2-isopropyl-2-oxazoline) (PIPOX), having 90 repeating units on the backbone is given in Figure 3.1. The TIC curve shows a single and a broad peak with a maximum at 445 °C. The pyrolysis mass spectrum recorded at 445 °C, during the thermal degradation of the polymer is also shown in the figure.

During the pyrolysis of PIPOX, peaks due to series of products with formula M_xH, M_xHCH_2, $M_xCH=CH_2$, M_xHNHCH_2, $M_xHN=COH$ or $M_xHNHC_2H_4$, M_xNCOCH_2, $M_xNCOCH_2CH_2$, $M_xHNHCOHC_3H_7$, $M_xH\text{-}CH_2$ and $[CH_2=CHN(COCH(CH_3)_2)$ $M_xCH_2]$ where x changes from 1 to 7 were detected and are summarized in Table 3.1. The base peak at 445 °C is at 181 Da $(CH_2=CHNCOC_3H_7)NCOCH=CH_2$).

The most intense peaks were due to protonated monomer (m/z=114 Da) and protonated oligomer ions (m/z=227, 340, 453, 566, 679, 792 Da). M_xNCOCH_2,

$M_xCH=CH_2$ and $M_xHNHCOHC_3H_7$ peaks were also quite significant.

Table 3.1: Series of products and their m/z values

SERIES of PRODUCTS	x	m/z Values
M_xH	1 to 7	114, 227, 340, 453, 566, 679, 792
M_xHCH_2	1 to 5	128, 241, 354, 467, 580
$M_xCH=CH_2$	1 to 5	140, 253, 366, 479, 592
M_xHNHCH_2	1 to 4	143, 256, 369, 482
$M_xHN=COH$ or $M_xHNHC_2H_4$	1 to 4	157, 270, 383, 496
M_xNCOCH_2	1 to 6	169, 282, 395, 508, 621, 734
$M_xNCOCH_2CH_2$	1 to 4	183, 296, 409, 522
$M_xHNHCOHC_3H_7$	1 to 6	201, 314, 427, 540, 653, 766
$M_xH\text{-}CH_2$	2 to 5	213, 326, 439, 552
$CH_2=CHN(COCH(CH_3)_2)M_xCH_2$	1 to 4	239, 352, 465, 578

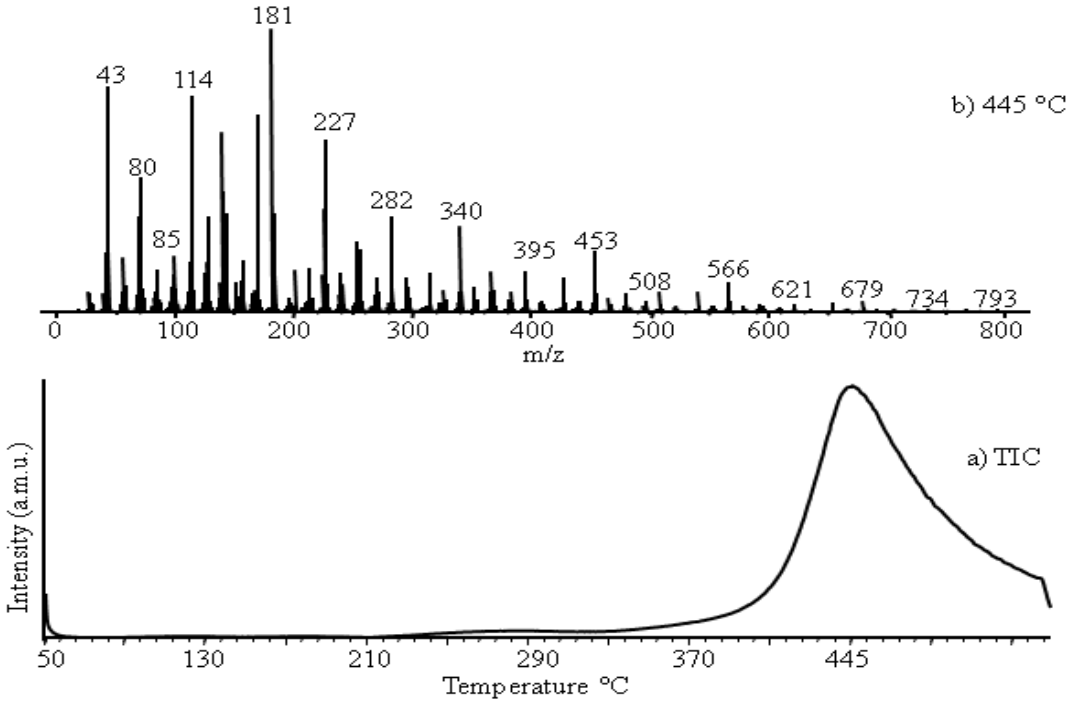

Figure 3.1: Pyrolysis mass data for PIPOX.

In Table 3.2 the relative intensities and m/z values for characteristic peaks recorded in the mass spectrum at 445 °C and the assignments are given.

In general, the fragmentation pattern observed pointed out a thermal decomposition mechanism via random cleavages.

Presence of protonated monomer and oligomers can be associated with a decomposition mechanism similar to McLafferty type rearrangement reaction as shown in Scheme 3.1.

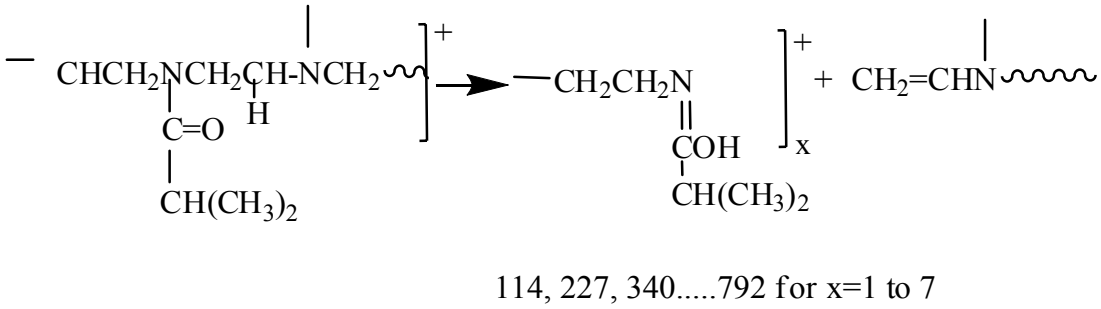

Scheme 3.1: Generation of protonated monomer and protonated oligomers.

It is known that thermal degradation products further dissociate in the mass spectrometer during ionization and all the fragments with the same mass to charge ratio make contributions to the intensities of the same peak in the mass spectrum. Due to this reason, direct pyrolysis mass spectra of polymers are usually very complex [41, 42]. Therefore, the trends in the single ion evolution profiles were used to determine the mechanism of thermal degradation or the source of the product.

Single ion evolution profiles of some selected products, namely $CH(CH_3)_2$ (m/z=43 Da), $NCOCH(CH_3)_2$ (m/z=85 Da), MH (m/z=114 Da), $CH=CHCH_2CH_2NCOC_3H_7$ (m/z=139 Da), $MN(CO)CH_2$ (m/z=169 Da), $(CH_2=CHNCOC_3H_7)NCOCH=CH_2$ (m/z=181 Da), DH (m/z=227 Da), $DN(CO)CH_2$ (m/z=282 Da), TriH (m/z=340 Da), $TriN(CO)CH_2$ (m/z=395 Da), TetH (m/z=453 Da), $TetN(CO)CH_2$ (m/z=508 Da), PH (m/z=566 Da), $PN(CO)CH_2$ (m/z=621 Da), HexH (m/z=679 Da) and $HexN(CO)CH_2$ (m/z=734 Da) are given in Figure 3.2. It can be noted from the figure that evolution profiles of all the products are almost identical and reached to maximum yield at 445 °C. Evolutions of monomer and low mass products, such as $CH(CH_3)_2$ (m/z=43 Da) were detected at low temperatures at around 250 °C indicating presence of low mass oligomers in the sample.

Analysis of samples involving different number of repeating units have been performed. Almost similar thermal degradation behaviour was observed for PIPOX50 and PIPOX90 where 50 and 90 were the number of repeating units.

Table 3.2: The relative intensities (RI) detected during the PIPOX pyrolysis and chemical assignments of the most intense and characteristic peaks in the mass spectrum of PIPOX at 445 °C.

m/z	RI	Assignment
43	813	$CH(CH_3)_2$
85	149	$NCOCH(CH_3)_2$
113	177	Monomer
114	779	MH
128	339	CH_2MH
139	645	$CH{=}CHCH_2CH_2NCOC_3H_7$
140	427	$MCH{=}CH_2$
143	351	$MHNHCH_2$
169	695	$MN(CO)CH_2$
181	1000	$(CH_2{=}CHNCOC_3H_7)NCOCH{=}CH_2$
183	351	$MNCOCH_2CH_2$
213	162	$MHN(COCH(CH_3)_2)CH_2$
227	611	DH
239	140	$CH_2{=}CHN(COCH(CH_3)_2)MCH_2$
241	100	CH_2DH
253	245	$DCH{=}CH_2$
256	218	$DHNH{=}CH_2$
270	118	$DHN{=}COH$, $DHNHCH_2CH_2$
282	335	$DN(CO)CH_2$
294	120	$CH_2{=}CHNCOC_3H_7MNCOCH{=}CH_2$
314	135	$DHNHCOHC_3H_7$
340	305	TriH
366	140	$TriCH{=}CH_2$
395	142	$TriN(CO)CH_2$
427	119	$TriHNHCOHC_3H_7$
453	216	TetH
479	69	$TetCH{=}CH_2$
482	42	$TetHNH{=}CH_2$
508	68	$TetN(CO)CH_2$
540	68	$TetHNHCOHC_3H_7$
566	105	PH
621	27	$PN(CO)CH_2$
653	29	$PHNHCOHC_3H_7$
679	39	HexH
734	8	$HexN(CO)CH_2$
792	10	HepH

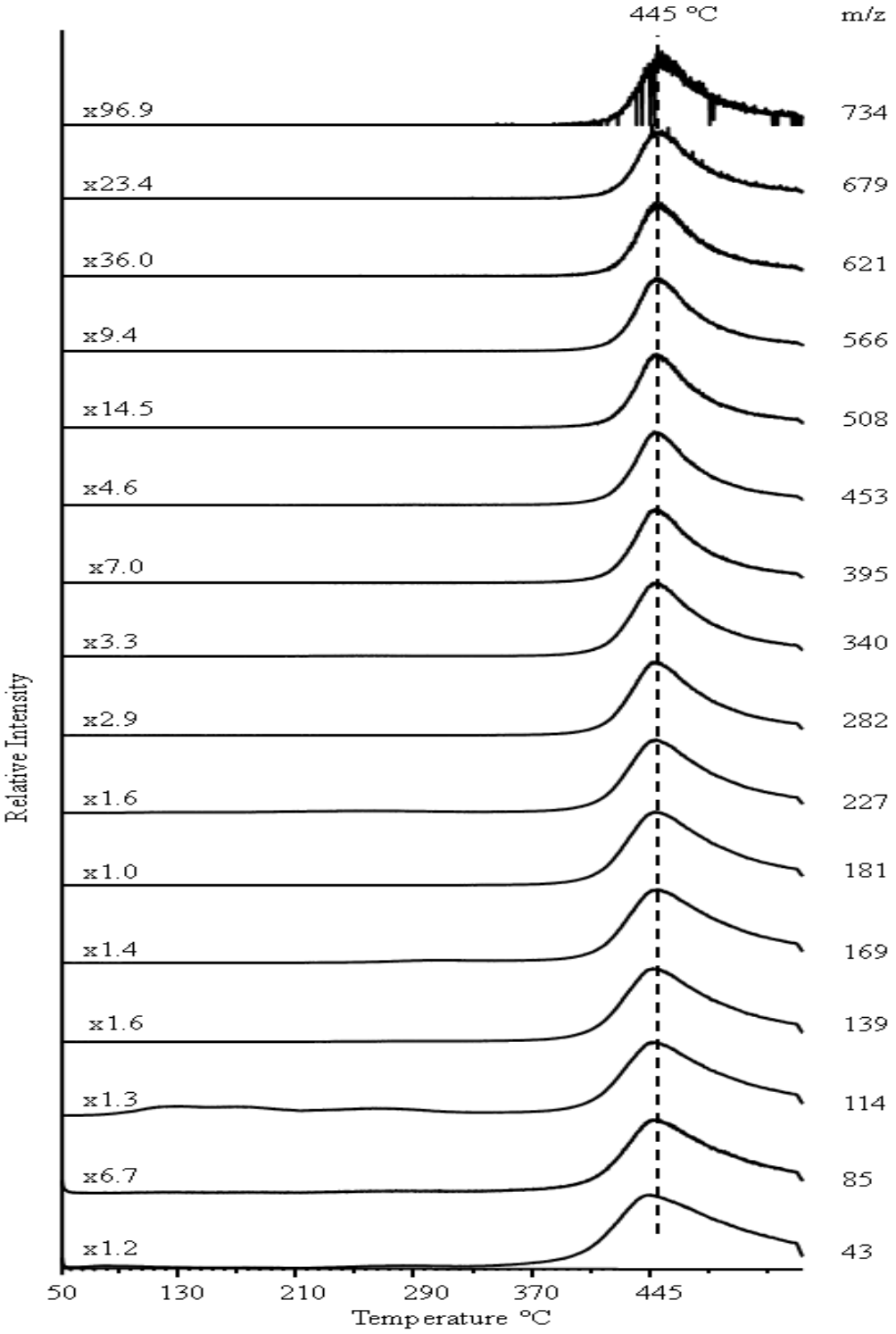

Figure 3.2: Single ion evolution pyrograms of some selected pyrolysis compounds obtained by direct pyrolysis of PIPOX.

3.2 Poly(2-(3-butenyl)-2-oxazoline) (PBOX)

The total ion current (TIC) curve of poly(2-(3-butenyl)-2-oxazoline) (PBOX) having 41 repeating units on the polymer backbone is given in Figure 3.3. A single and a broad peak was detected in the TIC curve. The pyrolysis mass spectra recorded at several temperatures during the pyrolysis of the polymer are also shown in the figure. At 300 °C, the base peak was at 55 Da due to C_4H_7 ion, whereas, at higher temperatures, the base peak was at 124 Da due to $[M-H]^+$. The pyrolysis mass spectra were dominated with peaks at m/z=69 Da [CH_2=CHNCO, C_5H_9], 82 Da [(OC=$CHCH_2CH$=CH_2, C_6H_{10}], 97 Da [$NCOC_4H_7$, C_7H_{13}] and 156 Da [$CH_3N(COCH_2)C_2H_4NHCOCH_2$]. Above 300 °C, peaks with m/z values higher than 200 Da were significantly weak.

In Table 3.3 the most intense and characteristic peaks recorded in the mass spectra at 300, 310, 405, 415 and 435 °C and the chemical assignments are summarized.

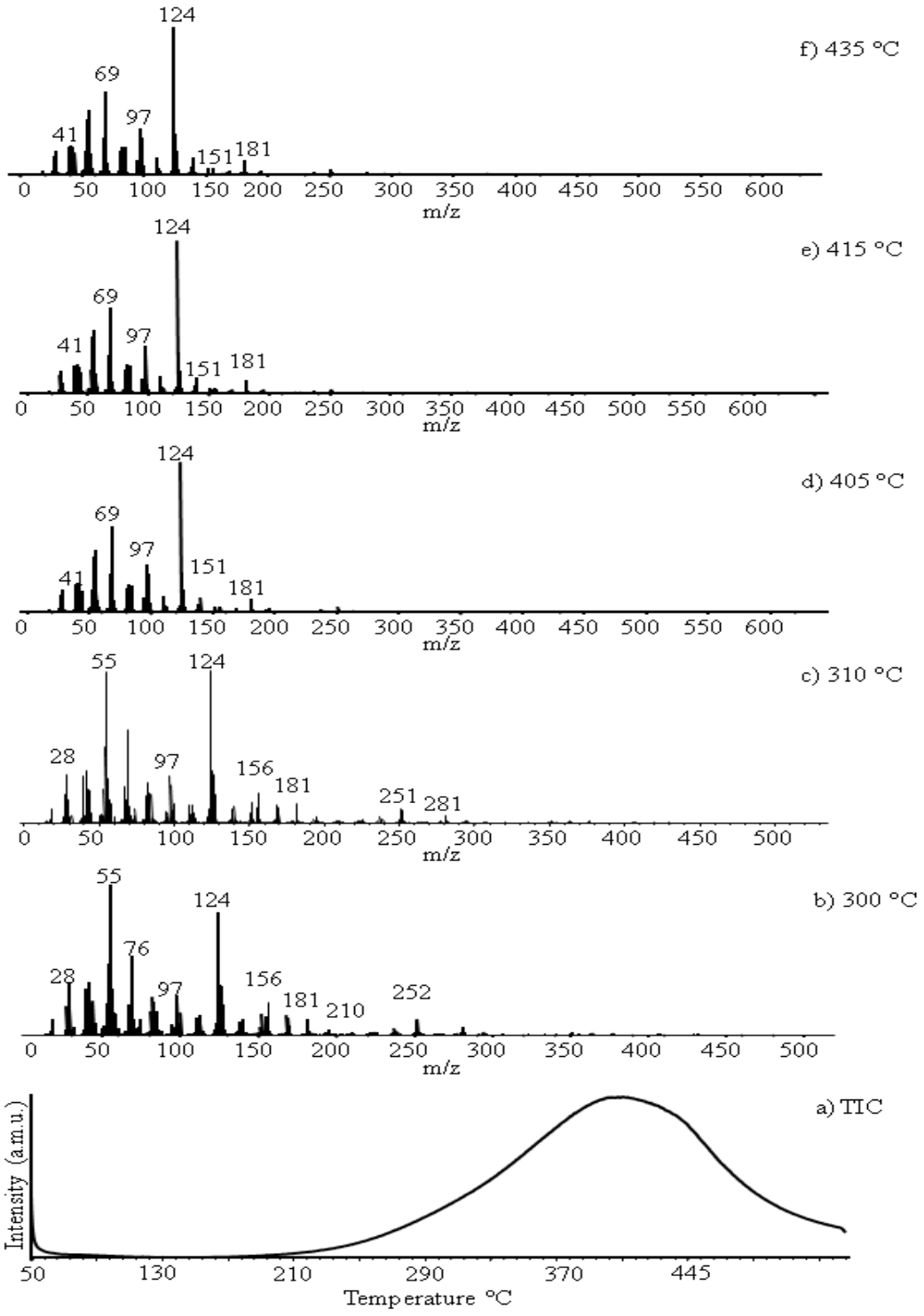

Figure 3.3: Pyrolysis mass data for PBOX.

Table 3.3: The relative intensities (RI) detected during the PBOX pyrolysis and chemical assignments of the most intense and characteristic peaks in the mass spectrum of PBOX at 300, 310, 405, 415 and 435 °C.

m/z	RI					Assignment
	300°C	310°C	405°C	415°C	435°C	
55	1000	986	414	416	436	$CH_2CH_2CHCH_2$
69	522	614	569	560	564	CH_2=CHNCO, C_5H_9
82	253	265	186	186	190	OC=$CHCH_2CH=CH_2$, C_6H_{10}
97	263	310	315	309	313	$NCOC_4H_7$, C_7H_{13}
110	113	120	103	109	114	$CHNCOC_4H_7$, $C_4H_6NCOCH_2$
124	810	1000	1000	1000	1000	M-H
125	331	346	261	263	275	Monomer
126	324	16	146	149	161	MH
140	102	112	95	101	113	$MHCH_2$, $(CH_2CH_2NCO)_2$
156	217	195	27	28	28	$CH_3N(COCH_2)C_2H_4NHCOCH_2$
169	116	104	26	28	31	$MHN=COH$, $MHNHCH_2CH_2$
181	108	124	86	87	100	$MNCOCH_2$, $CH_2NCOC_2H_4NCOC_4H_7$
237	44	43	15	15	17	$HMN(COC_4H_7)CH_2$
249	9	9	7	8	11	D-H
251	106	96	31	30	37	DH
280	19	20	10	12	14	$(CH_2CH_2NCO)_4$
281	54	50	9	9	10	$(CH_2CH_2NCO)_3CH_2CH_2N=COH$
374	0	0	1	1	1	Tri-H
376	11	11	7	7	7	TriH

Unlike what was detected for PIPOX, the main thermal decomposition products were M-H (124 Da), M (125 Da) and MH (126 Da) and the relative intensities of high mass products were less than 10% of the base peak $[M-H]^+$.

Single ion evolution profiles of some selected products, namely $C_4H_7(CH_2CH_2CHCH_2)$ (1-butenyl) (m/z=55 Da), CH_2=CHNCO, C_5H_9 (m/z=69 Da), OC=$CHCH_2CH$=CH_2, C_6H_{10} (m/z=82 Da), $NCOC_4H_7$, C_7H_{13} (m/z=97 Da), $CH_2NCOC_4H_7$, $C_4H_6NCOCH_2$ (m/z=110 Da), Monomer-H (m/z=124 Da), $MHCH_2$, $(CH_2CH_2NCO)_2$ (m/z=140 Da), $CH_3N(COCH_2)C_2H_4NHCOCH_2$ (m/z=156 Da), MHN=COH, $MHNHCH_2CH_2$ (m/z=169 Da), $MNCOCH_2$, $CH_2NCOC_2H_4NCOC_4H_7$ (m/z=181 Da), $HMN(COC_4H_7)CH_2$ (m/z=237 Da), DH (m/z=251 Da), $(CH_2CH_2NCO)_4$ (m/z=280 Da), $(CH_2CH_2NCO)_3CH_2CH_2N$=COH (m/z=281 Da) and TriH (m/z=376 Da) are shown in Figure 3.4. Although, the TIC curve showed a single peak, four different maxima were recorded in the single ion pyrograms. Analysis of the single ion evolution profiles of products generated during the pyrolysis pointed out significant differences. Taking into account the trends observed in the evolution profiles four groups of products can be differentiated.

Low temperature evolutions at around 300 and 310 °C can be attributed to the decomposition of low mass oligomers.

[M-H] (124 Da) and low mass fragments were maximized at around 405 °C. On the other hand, high mass products showed a low temperature peak or a shoulder at around 310 °C and a high temperature peak at around 435 °C in their single ion pyrograms.

Fragments that can be associated with products generated by cleavage of side chains showed maximum yield at 415 °C.

The main difference between PIPOX and PBOX is the group substituted to carbonyl group. It may be thought that during the pyrolysis, polymerization of the unsaturated butenyl group took place yielding a crosslinked structure. Generation of such linkages would inhibit production of oligomers.

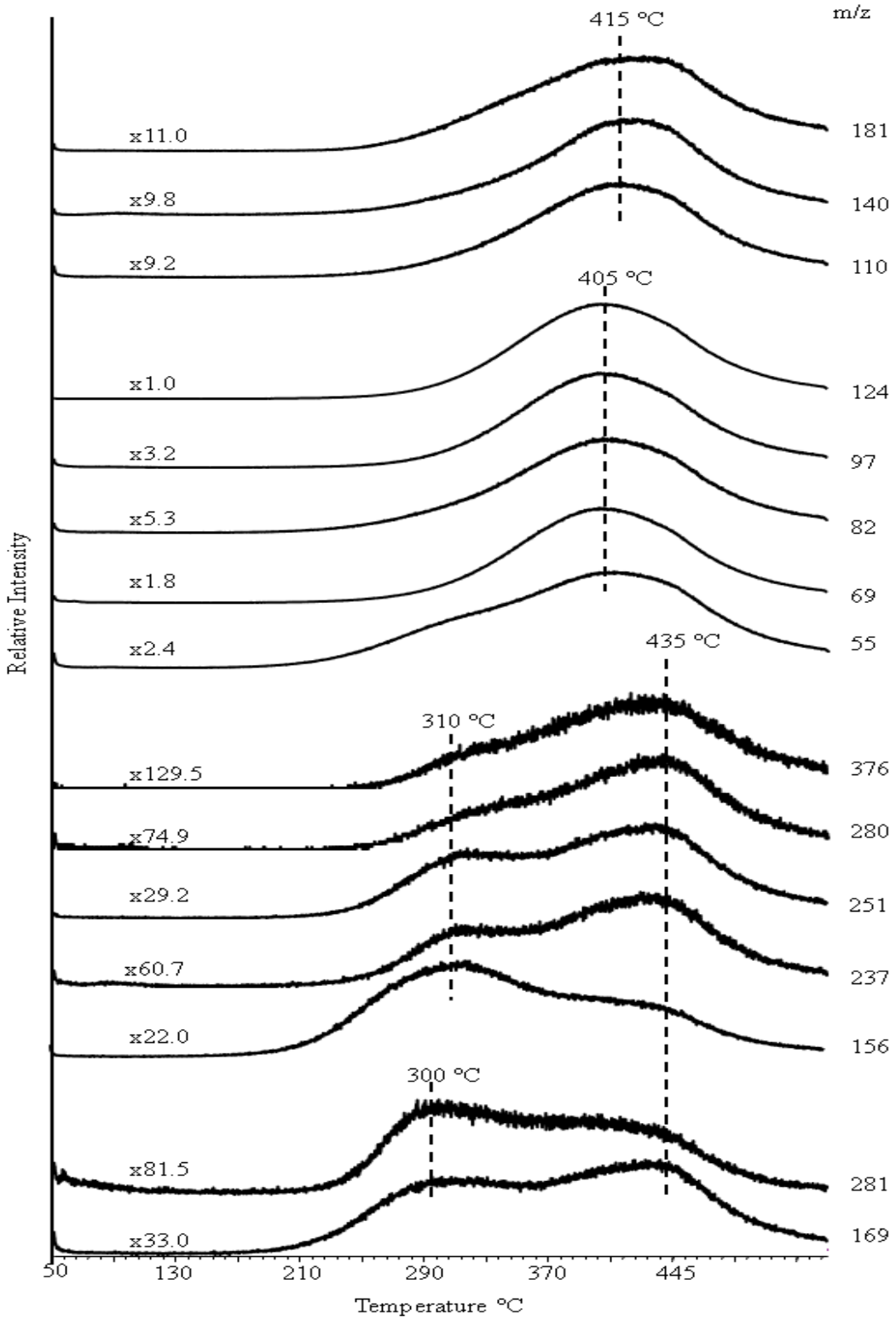

Figure 3.4: Single ion evolution pyrograms of some selected pyrolysis compounds obtained by direct pyrolysis of PBOX.

3.3 Poly(2-(3-butenyl)-2-oxazoline) modified with 1H,1H,2H,2H-perfluoro-octanethiol (PBOX-Perf)

Three peaks were detected in the TIC curve of PBOX-Perf given in Figure 3.5. The pyrolysis mass spectra recorded at 67, 310, 332 and 445 °C during the thermal degradation of the polymer are also included in the figure. The base peak at 67 °C was 205 Da whereas, at 310, 332 and 445 °C, the base peak was at 158 Da. The broad evolution profile with a maximum at around 332 °C indicated a significant decrease in the thermal stability of PBOX upon modification with 1H, 1H,2H,2H-perfluoro-octanethiol. The intense peaks at m/z=47 Da [C_4H_7], 69 Da [CF_3, CH_2=CHNCO], 87 Da [$CH_2CHCH_2SCH_2$,C_4H_7S, $CH_2CH_2CH_2CH$=S], 98 Da [$CH_2CH_2NCO(CH_2)_2$, $NCO(CH_2)_4$,CH_2=$NCO(CH_2)_3$], 126 Da [$CH_2CH_2NCOCH_2$ $CH_2CH_2CH_2$], 407 Da [$CF_3(CF_2)_5CH_2CH_2SCH_2CH_2$] and 463 Da [$CF_3(CF_2)_5$ CH_2CH_2S=$CH_2CH_2CH_2CH_2CO$] were detected.

In Table 3.4, the most intense and characteristic peaks recorded in the mass spectra at 67, 310, 332 and 445 °C and the assignments made are summarized. The peaks detected at around 332 and 445 °C were almost identical but differences in the relative intensities were noted.

Single ion evolution profiles of some selected products, namely CH_2SH (m/z=47 Da), $C_4H_7(CH_2CH_2CHCH_2)$ (1-butenyl) (m/z=55 Da), CF_3, CH_2=CHNCO (m/z=69 Da), $CH_2CHCH_2SCH_2$, $CH_2CHCH_2CH_2S$, $CH_2CH_2CH_2CH$=S (m/z=87 Da), $CH_2CH_2NCO(CH_2)_2$, $NCO(CH_2)_4$, CH_2=$NCO(CH_2)_3$ (m/z=98 Da), CH_2CH_2NCO $CH_2CH_2CH_2CH_2$ (m/z=126 Da), $CH_2NCOCH_2CH_2CH_2CH_2SCH_2$ (m/z=158 Da), $CH_2CH_2NCO(CH_2)_4SCH_2$, $CH_2NCO(CH_2)_4SCH_2CH_2$ (m/z=172 Da), CH_2CH_2N $(CO(CH_2)_4)SCH_2CH_2$ (m/z=186 Da), CF_2=$CFCF_2CH_2CH_2SCH_2$ (m/z=205 Da), $CF_3(CF_2)_3$ (m/z=219 Da), $CF_3(CF_2)_4CFH(CH_2)_2SS$, $(CF_2)_6(CH_2)_2SSH$, $CF_3(CF_2)_5$ $(CH_2)_2SCH_2$ (m/z=393 Da), $CF_3(CF_2)_5CH_2CH_2SCH_2CH_2$ (m/z=407 Da), $CF_3(CF_2)_5$ $CH_2CH_2SCH_2CH_2CH_2CH_2$ (m/z=435 Da), $CF_3(CF_2)_5CH_2CH_2S$=CH_2CH_2 CH_2CH_2CO (m/z=463 Da), MH (m/z=506 Da), $MHNCH_2$ (m/z=534 Da),

$MHNCOHCH_2$ (m/z=563 Da) and $CF_3(CF_2)_5(CH_2)_2SSCH_2CH_2(CF_2)_5CF_3$ (m/z=758 Da) are shown in Figure 3.6.

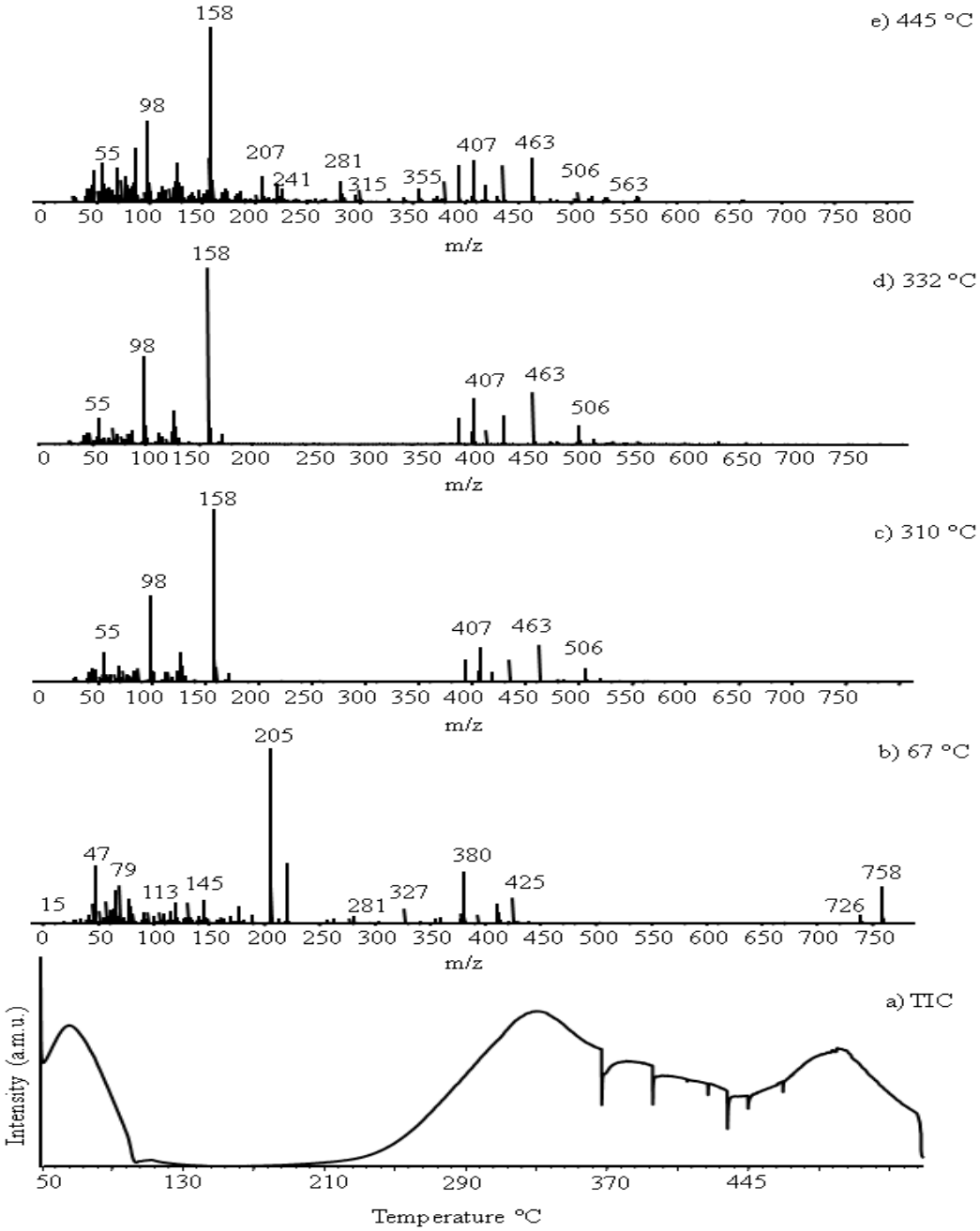

Figure 3.5: The pyrolysis mass data for PBOX-Perf.

Table 3.4: The relative intensities (RI) detected during the PBOX-Perf pyrolysis and chemical assignments of the most intense and characteristic peaks in the mass spectrum of PBOX-Perf at 67, 310, 332 and 445 °C.

m/z	RI				Assignment
	67°C	310°C	332°C	445°C	
47	328	74	66	185	CH_2SH
55	33	173	152	226	$CH_2CH_2CHCH_2$
65	191	44	40	71	C_4H_3N
69	220	99	93	199	CF_3, CH_2=CHNCO
77	137	45	42	151	CF_2CH=CH_2, C_6H_5
79	97	36	34	102	$CHF_2CH_2CH_2$, $CF_2CH_2CH_3$, C_6H_7
87	6	82	78	313	$CH_2CHCH_2SCH_2$, C_4H_7S, $CH_2CH_2CH_2CH$=S
91	67	5	5	19	$CFCH_2CH_2S$, HCF=$CFCH_2CH_2$, C_7H_7
98	2	503	495	467	$C_2H_4NCO(CH_2)_2$, $NCO(CH_2)_4$, CH_2=$NCO(CH_2)_3$
105	62	2	2	8	$CFCH_2CH_2SCH_2$, $C_6H_5CH_2CH_2$
112	4	63	66	91	CH_2=$NCO(CH_2)_4$
126	5	176	192	228	$CH_2CH_2NCO(CH_2)_4$
131	120	36	37	94	CF_2CFCF_2
145	133	6	6	24	CF_2CF_2CF=CH_2
158	8	1000	1000	1000	$CH_2NCO(CH_2)_4SCH_2$
169	38	18	20	55	$CF_3(CF_2)_2$
172	14	54	58	78	$CH_2CH_2NCO(CH_2)_4SCH_2$,$CH_2NCO(CH_2)_4SCH_2CH_2$
177	102	2	2	19	$CF_2CF_2CF_2CH$=CH_2
186	0	8	10	64	$C_2H_4NCO(CH_2)_4SC_2H_4$,$C_2H_4NCO(CH_2)_4SCH_2CH_2$
205	1000	1	1	14	CF_2=$CFCF_2CH_2CH_2SCH_2$
219	17	3	3	16	$CF_3(CF_2)_3$
263	29	5	5	18	$CF_3CF_2CF_2CF_2CF$=CH
281	42	7	7	121	$CF_3CFCF(CF_2)_3$, $(CH_2CH_2NCO)_3CH_2CH_2N$=COH
327	85	4	5	25	$CF_3(CF_2)_4CFCHCH_2$
359	37	2	2	15	$CF_3(CF_2)_4CFCHCH_2S$
380	294	9	13	123	$CF_3(CF_2)_5CH_2CH_2SH$
393	48	129	148	211	$C_5F_{11}CFHC_2H_4SS$, $C_6F_{12}C_2H_4SSH$, $C_6F_{13}C_2H_4SCH_2$
407	6	205	259	245	$CF_3(CF_2)_5CH_2CH_2SCH_2CH_2$
411	115	3	3	5	$CF_3(CF_2)_5CH_2CH_2SS$
421	15	5	7	11	$CF_3(CF_2)_5CH_2CH_2SCH_2CH_2CH_2$
425	148	1	1	3	$CF_3(CF_2)_5CH_2CH_2SSCH_2$
435	0	128	165	215	CF_3 $(CF_2)_5CH_2CH_2SCH_2CH_2CH_2CH_2$
439	12	2	2	3	$CF_3(CF_2)_5CH_2CH_2SSCH_2CH_2$
463	1	218	298	253	$CF_3(CF_2)_5CH_2CH_2S$=$CH_2CH_2CH_2CH_2CO$
489	9	1	1	5	$CF_3(CF_2)_5CH_2CH_2SSCH_2CH_2CF_2$
491	1	0	0	3	$CF_3(CF_2)_5CH_2CH_2S$=$(CH_2)_4CONCH_2$
506	0	79	106	57	MH
534	0	2	3	32	$MHNCH_2$
563	0	3	5	38	$MHNCOHCH_2$
758	212	0	0	1	$CF_3(CF_2)_5CH_2CH_2SSCH_2CH_2(CF_2)_5CF_3$

At around 67 °C, evolution of $(CF_3(CF_2)_5(CH_2)_2S)_2$ (m/z=758 Da) was detected together with the starting material $CF_3(CF_2)_5(CH_2)_2SH$ (m/z=380 Da). Thus, it can be concluded that the starting material $CF_3(CF_2)_5(CH_2)_2SH$ has been dimerized by the loss of H during the synthesis and/or storage. The evolution of $CF_3(CF_2)_5(CH_2)_2SH$, the starting material, was completed below 100 °C. Evolution of dimer was recorded in a broader temperature range.

Monomer peak at 506 Da reached maximum intensity at around 332 °C. A second maximum pointing out the presence of units with higher thermal stability was obtained in the pyrolysis mass spectra recorded at around 445 °C. The peaks in the pyrolysis mass spectra recorded at around 332 and 445 °C were almost identical but differences in the relative intensities were noted.

Single ion evolution profiles of most of the decomposition products again showed two maxima. Evolution of 55 Da fragment at slightly lower temperatures may be an indication of presence of unreacted three butenyl groups. Most of the products reached maximum yield at around 332 °C. Only few products such as 186, 534 and 563 Da fragments showed maxima at around 445 °C in their single ion pyrograms. These products are either high mass products involving monomer or products such as 186 Da fragment. 186 Da peak may be due to $CH_2CH_2N(CO(CH_2)_4)SCH_2CH_2$ or $CH_2CH_2N(CO(CH_2)_4SCH_2)CH_2$. The second product can only be generated by decomposition of an oligomer or a polymer chain. Again the products $MHNCH_2$ and $MHNCOHCH_2$ at 534 and 563 Da respectively were necessarily produced by decomposition of an oligomer or a polymer chain. On the other hand, all the products that showed maxima at 332 °C can be generated by decomposition of the monomer unit.

Thus, it can be concluded that degradation of polymer backbone occurred in the final stages of pyrolysis, whereas decomposition of side chains took place readily at around 330 °C.

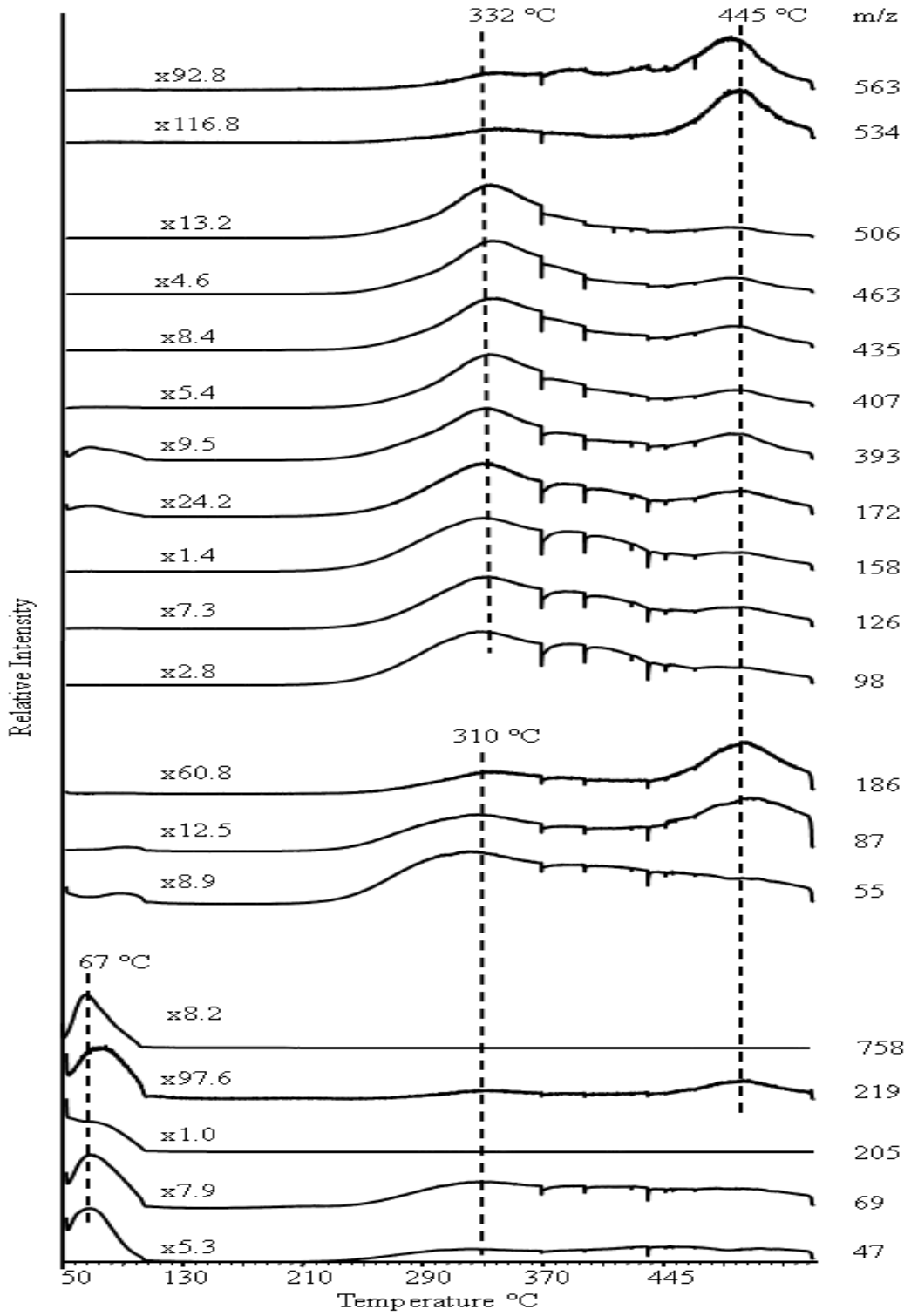

Figure 3.6: Single ion evolution pyrograms of some selected pyrolysis compounds obtained by direct pyrolysis of PBOX-Perf.

3.4 Poly(2-(3-butenyl)-2-oxazoline) modified with Thio-β-D-glucose derivative (PBOX-Sug)

The total ion current (TIC) curve of PBOX-Sug is given in Figure 3.7. Three overlapping peaks were detected in the TIC curve with maxima at 320, 410 and 445 °C. The pyrolysis mass spectra recorded at the peak maxima are also given in figure 3.7. The base peak at 310, 320, 410 and 445 °C in the pyrolysis mass spectra recorded during the whole process was at 60 Da that can be attributed to either CH_2CH_2S or $(CHOH)_2$. The intense peaks at m/z=45 Da [CH=S], 55 Da [$CH_2CH_2CHCH_2$], 87 Da [$CH_2CHCH_2CH_2S$], 116 Da [$CO(CH_2)_4S$, $CH_2CHCH_2CH_2SCHO$], 123 Da [$CH_2CHNCOCHCH_2CHCH_2$, $(CH_2CHN)_3$] and 135 Da [HSCHOCHOHCHOHCH, $C_7H_9N_3$] were detected.

High mass product peaks were almost absent. Contrary to PIPOX, PBOX and PBOX-Perf, no monomer peak was detected for this sample.

In Table 3.5 the most intense and characteristic peaks recorded in the mass spectra at 310, 320, 410 and 445 °C and the assignments made are summarized.

Single ion evolution profiles of some selected products, namely CH=S (m/z=45 Da), CH_2CH_2S, $(CHOH)_2$ (m/z=60 Da), $NCOCHCH_2$ (m/z=69 Da), $NCOCH_2CH_2$ (m/z =70 Da), CHOHCHOHCH (m/z=73 Da), $CH_2CHCH_2CH_2S$ (m/z=87 Da), $NCOCH_2$ CH_2CHCH_2 (m/z=97 Da), $CH_2CH_2NCOCH_2CH_2$, $NCO(CH_2)_4$ (m/z=98 Da), SCHCHOHCHOH (m/z=105 Da), $CH_2OHCHOHCH_2S$, $(CH_2CHN)_2CCH$ (m/z =107 Da), $CO(CH_2)_4S$, $CH_2CHCH_2CH_2SCHO$ (m/z=116 Da), $CH_2SCHCHOH$ CHOH, $C_7H_7N_2$ (m/z=119 Da), $CH_2CHNCOCHCH_2CHCH_2$, $(CH_2CHN)_3$ (m/z=123 Da), $(CHOH)_4CH$, $C_8H_9N_2$ (m/z=133 Da), HSCHOCHOHCHOHCH, $C_7H_9N_3$ (m/z=135 Da), $CH_2CH_2SCHOCHOHCHOH$, $C_8H_{11}N_3$, $(CH_2CHN)_3CHCH$ (m/z=149 Da) and $(CH_2CH_2NCO)_3CH_2CH_2N{=}COH$ (m/z=281 Da) are shown in Figure 3.8.

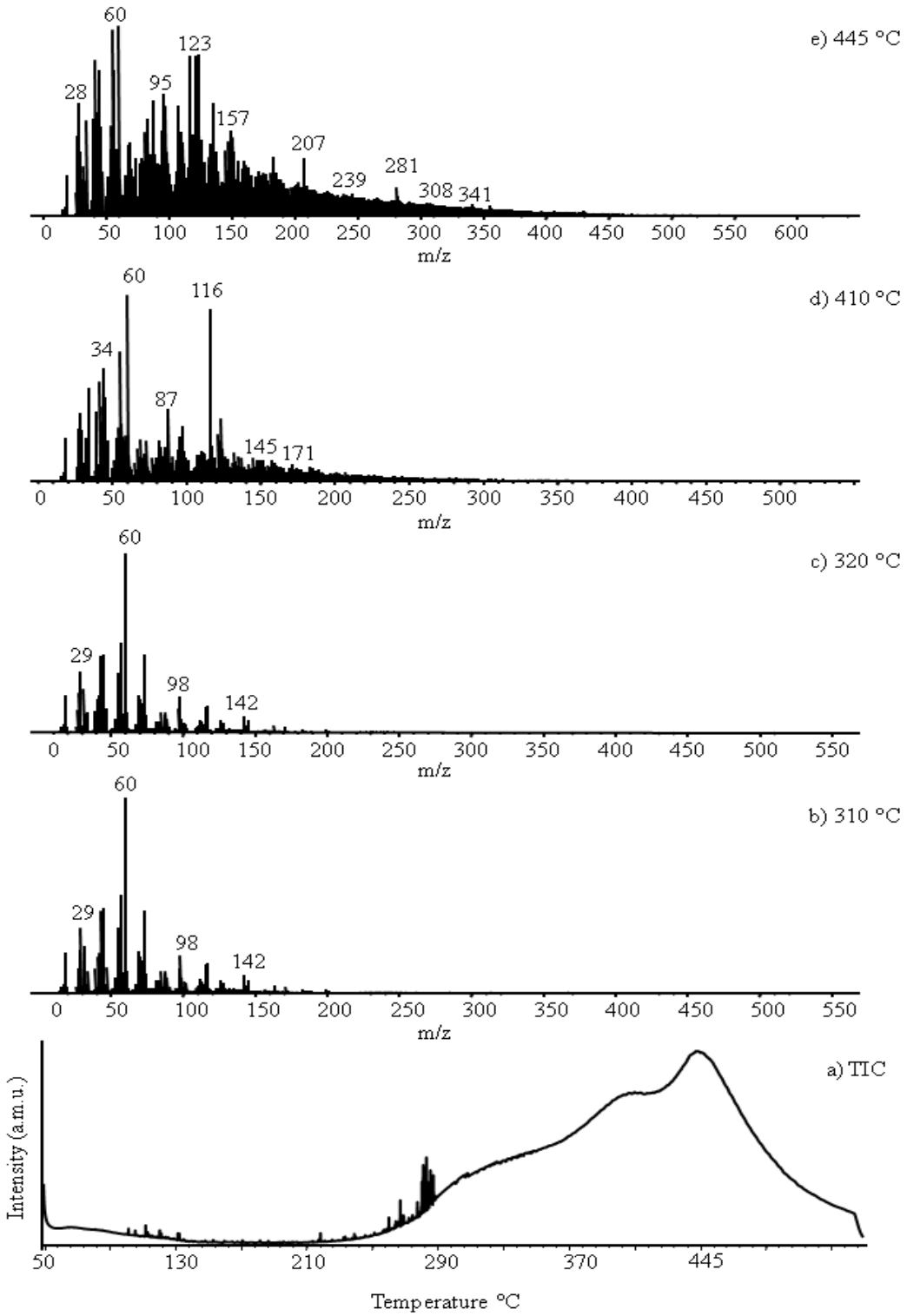

Figure 3.7: Pyrolysis mass data for PBOX-Sug.

Table 3.5: The relative intensities (RI) detected during the PBOX-Sug pyrolysis and chemical assignments of the most intense and characteristic peaks in the mass spectrum of PBOX-Sug at 310, 320, 410 and 445 °C.

m/z	RI				Assignment
	310°C	320°C	410°C	445°C	
18	165	207	238	218	H_2O
43	373	427	403	514	OHCHCH
45	347	433	453	471	CH=S
55	282	331	708	982	$CH_2CH_2CHCH_2$
60	1000	1000	1000	1000	CH_2CH_2S, $(CHOH)_2$
69	191	211	231	389	$NCOCHCH_2$
70	185	188	133	251	$NCOCH_2CH_2$
73	424	432	224	303	CHOHCHOHCH
86	26	34	87	212	CHCHOHCHOHCH
87	77	101	394	609	$CH_2CHCH_2CH_2S$
97	112	131	294	578	$NCOCH_2CH_2CHCH_2$
98	169	197	176	342	$CH_2CH_2NCOCH_2CH_2$, $NCO(CH_2)_4$
105	10	12	72	166	SCHCHOHCHOH
107	9	14	146	582	$CH_2OHCHOHCH_2S$, $(CH_2CHN)_2CCH$
116	107	140	912	846	$CO(CH_2)_4S$, $CH_2CHCH_2CH_2SCHO$
117	120	152	197	277	$(CH_2)_4SCHO$
119	13	15	129	431	$CH_2SCHCHOHCHOH$, $C_7H_7N_2$
123	16	23	348	849	$CH_2CHNCOCHCH_2CHCH_2$,$(CH_2CHN)_3$
133	9	10	114	382	$(CHOH)_4CH$, $C_8H_9N_2$
135	17	21	136	596	HSCHOCHOHCHOHCH, $C_7H_9N_3$
142	78	93	97	182	$CH_2NCOCHCHCH_2CH_2S$
149	7	8	115	453	$CH_2CH_2SCHOCHOHCHOH$, $C_8H_{11}N_3$, $(CH_2CHN)_3CHCH$
281	2	2	26	153	$(CH_2CH_2NCO)_3CH_2CH_2N{=}COH$

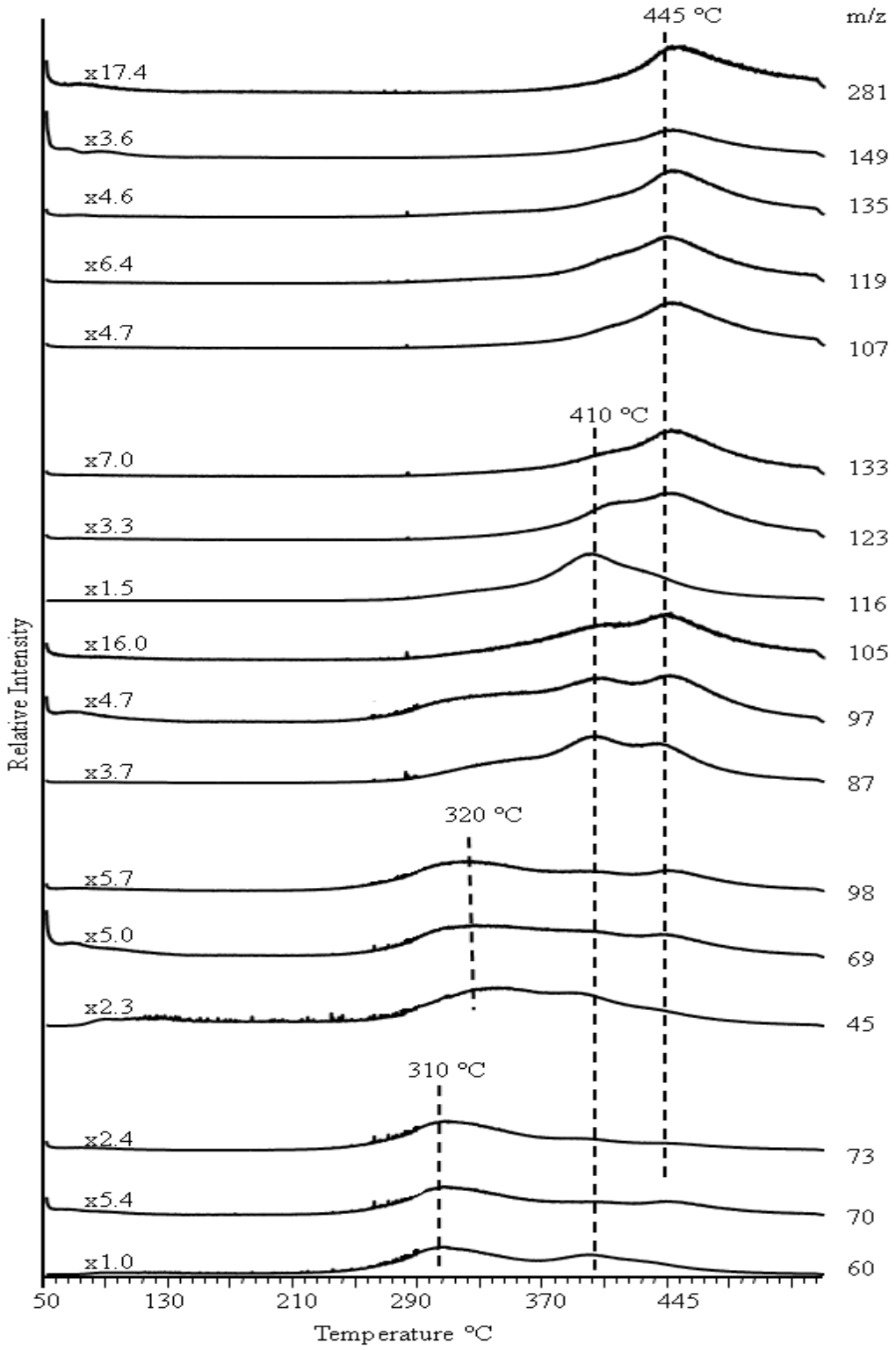

Figure 3.8: Single ion evolution pyrograms of some selected pyrolysis compounds obtained by direct pyrolysis of PBOX-Sug.

Product yields were maximized at different temperatures indicating the presence of units and/or chains with different stabilities. Low mass fragments that can be associated with decomposition of cyclic end groups maximized at around 310 °C. Products generated by loss of glucose units and cleavage of the main chain were maximized at 410 and 445 °C, respectively.

The trends detected in the evolution profiles indicated that the decomposition of polymer was started by cleavage of glucose units. This step was followed by loss of side chains. The high temperature evolutions were associated with the decomposition of polymer backbone, generated upon loss of side chains.

3.5 Poly(2-(3-butenyl)-2-oxazoline) modified with 3-mercapto-1,2 propanediol (PBOX-Thiop)

The total ion current (TIC) of PBOX-Thiop and pyrolysis mass spectra recorded at 80, 410, 425 and 445 °C are given in Figure 3.9. The base peak at 80 °C is 205 Da, it is 43 Da at 410 °C and 55 Da at 425 °C, whereas, at 445 °C, the base peak is at 123 Da. Peaks at m/z=42 Da [$(CH_2)_3$], 73 Da [CH_2SCHCH_2, CH_2SCH_2CH, SCH_2CHCH_2], 87 Da [$CH_2CHCH_2SCH_2$, $CH_2CHCH_2CH_2S$, $CH_2CH_2CH_2CH{=}S$], 101 Da [$CH_2CHCH_2CH_2SCH_2$], 159 Da [$C_2H_4NCO(CH_2)_4SH$, $CH_2NCOH(CH_2)_4$ SCH_2] and 190 Da [$CO(CH_2)_4SCH_2CHOHCHOH$, $COCH(CH_2)_3SCH_2CHOH$ CH_2OH] were detected as intense peaks.

There are three peaks in the TIC curve of PBOX-Thiop as in the case of PBOX-Perf TIC curves. However, for PBOX-Thiop, the TIC curve was maximized at significantly higher temperatures compared to PBOX-Perf and PBOX-Sug. Evolution of low mass fragments indicating the cleavage of the side chains was dominant at around 400 °C. Products pointing out decomposition of the main chain were again maximized at around 445 °C.

Contrary to PBOX-Sug, monomer peak was detected for this sample as in the case of PBOX-Perf.

In Table 3.6 the most intense and characteristic peaks recorded in the mass spectra at 80, 410, 425 and 445 °C and the assignments made are summarized.

Single ion evolution profiles indicated a more homogeneous structure than PBOX-Perf. Single ion evolution profiles of some selected products, namely $(CH_2)_3$ (m/z =42 Da), $CH_2CH_2CHCH_2$ (m/z=55 Da), CH_2CH_2S, $(CHOH)_2$ (m/z=60 Da), CH_2SCHCH (m/z=72 Da), CH_2SCHCH_2, CH_2SCH_2CH, SCH_2CHCH_2 (m/z=73 Da), $OCCH_2CH_2CHCH_2$, $CH_2COCHCH_2CH_2$ (m/z=83 Da), CH_2SCH_2CHOH (m/z=90 Da), $CH_2CHCH_2CH_2SCH_2$ (m/z=101 Da), $OCCH_2CH_2CH_2CH_2S$ (m/z=116 Da), $CH_2CHNCOCHCH_2CHCH_2$ (m/z=123 Da), $COCH_2CH_2CH_2SCHCHOH$, $NHCO(CH_2)_4SCH_2$, $CH_2NCO(CH_2)_4SH$, $NCOH(CH_2)_4SCH_2$ (m/z=145 Da), $CH_2CH NCO(CH_2)_4S$, $CH_2CH_2NCO(CH_2)_3CH=S$ (m/z=157 Da), $CH_2CHNCO(CH_2)_4SCH_2$ (m/z=171 Da), $CO(CH_2)_4SCH_2CHOHCHOH$, $COCH(CH_2)_3SCH_2CHOHCH_2OH$ (m/z=190 Da), $CH_2CHNCO(CH_2)_4SCH_2CHOH$ (m/z=201 Da), $NCO(CH_2)_4SCH_2 CHOHCH_2OH$ (m/z=205 Da), $CH_3NCO(CH_2)_4SCH_2CHOHCH_2OH$, $CH_2NCOH(CH_2)_4SCH_2CHOHCH_2OH$ (m/z=220 Da), Monomer (m/z=233 Da) and MCH_2 (m/z=247 Da) are shown in Figure 3.10.

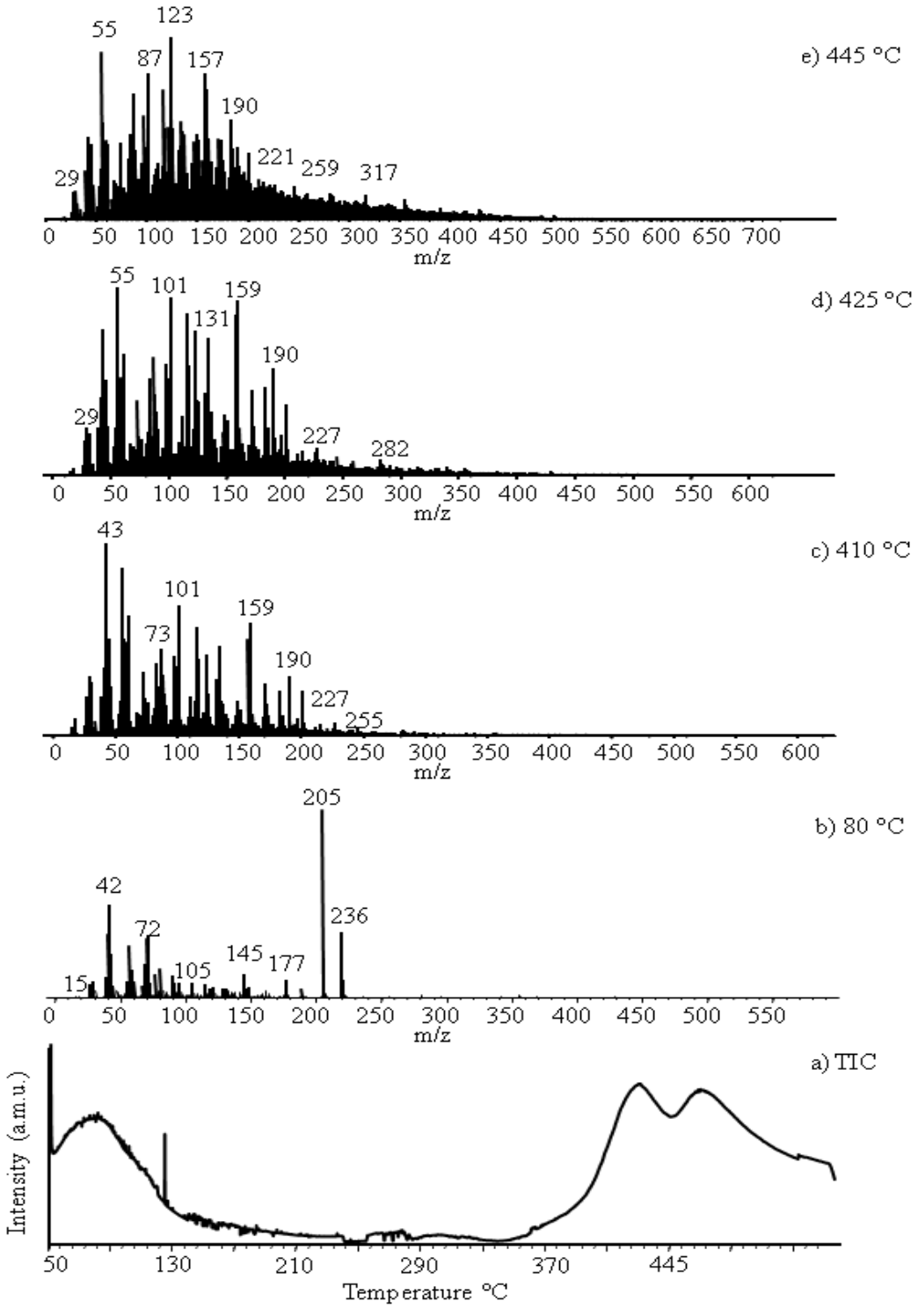

Figure 3.9: Pyrolysis mass data for PBOX-Thiop.

Table 3.6: The relative intensities (RI) detected during the PBOX-Thiop pyrolysis and chemical assignments of the most intense and characteristic peaks in the mass spectrum of PBOX-Thiop at 80, 410, 425 and 445 °C.

m/z	RI				Assignment
	80°C	410°C	425°C	445°C	
42	487	247	282	279	$(CH_2)_3$
43	227	1000	779	417	$CH(CH_3)_2$
55	89	868	1000	926	$CH_2CH_2CHCH_2$
60	26	253	371	443	CH_2CH_2S, $(CHOH)_2$
72	328	93	116	139	CH_2SCHCH
73	75	328	400	419	CH_2SCHCH_2, CH_2SCH_2CH, SCH_2CHCH_2
83	37	374	513	473	$OCCH_2CH_2CHCH_2$, $CH_2COCHCH_2CH_2$
87	19	448	632	697	$C_3H_5SCH_2$, $CH_2CH(CH_2)_2S$, $(CH_2)_3CH{=}S$
90	112	217	243	159	CH_2SCH_2CHOH
97	29	412	592	575	$CH_2NCOCH_2CHCH_2$
98	14	225	329	360	$CH_2NCOCH_2CH_2CH_2$
101	17	675	944	802	$CH_2CHCH_2CH_2SCH_2$
116	26	561	865	721	$OCCH_2(CH_2)_3S$
121	57	122	242	509	$CH_2SCH_2CHOHCH_2OH$
123	27	417	770	1000	$CH_2CHNCOCHCH_2CHCH_2$
145	129	61	149	313	$CO(CH_2)_3SCHCHOH$, $NHCO(CH_2)_4SCH_2$, $CH_2NCO(CH_2)_4SH$, $NCOH(CH_2)_4SCH_2$
149	57	111	257	471	$(CH_2)_3SCH_2CHOHCH_2OH$
157	19	505	856	807	$CH_2CHNCO(CH_2)_4S$, $C_2H_4NCO(CH_2)_3CH{=}S$
159	25	583	934	716	$C_2H_4NCO(CH_2)_4SH$, $CH_2NCOHC_4H_8SCH_2$
171	6	271	450	447	$CH_2CHNCO(CH_2)_4SCH_2$
173	7	104	262	441	$C_2H_4NCOH(CH_2)_4SCH_2$
175	17	59	153	332	$HNCO(CH_2)_4SCH_2CHOH$
177	103	61	134	265	$H_2NCO(CH_2)_4SCH_2CH_2OH$
190	10	309	568	399	$COC_4H_8SCH_2(CHOH)_2$, $COCHC_3H_6SCH_2CHOHCH_2OH$
191	10	75	196	293	$CO(CH_2)_4SCH_2CHOHCH_2OH$
201	2	232	379	365	$CH_2CHNCO(CH_2)_4SCH_2CHOH$
205	100	26	69	164	$NCO(CH_2)_4SCH_2CHOHCH_2OH$
220	350	14	44	131	$CH_3NCOC_4H_8SCH_2CHOHCH_2OH$, $CH_2NCOH(CH_2)_4SCH_2CHOHCH_2OH$
233	1	23	79	158	M
235	1	14	46	126	$CH_3CH_2NCOH(CH_2)_4SCH_2CHOHCH_2OH$
247	1	17	51	143	MCH_2

Low temperature evolutions were maximized at two different temperatures; 67 and 80 °C. In this region evolutions of unreacted and/or dissociated monomer during transport and/or storage were detected. Furthermore, evolution of $RSCH_2CHOHCH_2OH$ units indicating presence of unreacted reactants was observed.

Low mass fragments with m/z values 55 Da and 73 Da maximized at around 410 and 425 °C respectively were associated with decomposition of side chains. Main decomposition was again recorded at around 445 °C. Besides the evolution of fragments indicating loss of side chains, products due to decomposition of the main chain was recorded in this region.

Evolution profiles of monomer and higher mass fragments showed maxima at 445 °C. The trends in the evolution profiles pointed out that thermal decomposition again started by lose of side chains as in case of PBOX-Sug and PBOX-Perf. However, unlike what was observed for PBOX-Sug and PBOX-Perf, the temperature region where the loss of side chains occurred was very close to the region where decomposition of the main chain was detected indicating that thermal stability of side chains were significantly higher for PBOX-Thiop.

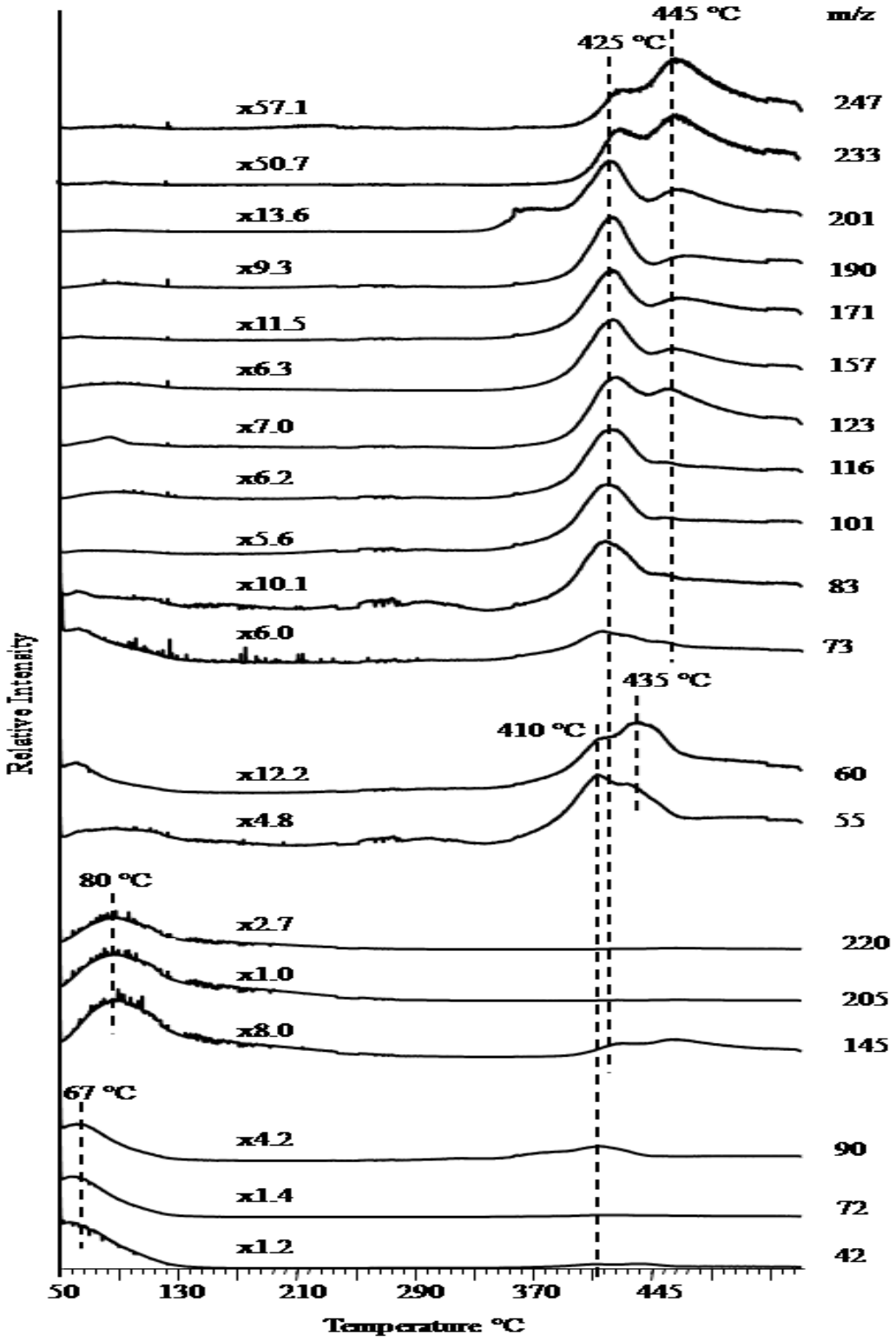

Figure 3.10 Single ion evolution pyrograms of some selected pyrolysis compounds obtained by direct pyrolysis of PBOX-Thiop.

3.6 Poly(2-(3-butenyl)-2-oxazoline) modified with mixture of 99% Thio-β-D-glucose derivative and 1% 1H,1H,2H,2H-perfluoro-octanethiol (PBOX-SP1)

The total ion current (TIC) curve of PBOX-SP1 is given in Figure 3.11. Two peaks were detected with maxima at 400 and 445 °C. The pyrolysis mass spectra recorded at 380, 400, 425 and 445 °C are also shown in Figure 3.11. The base peak at 380 and 400 °C was at 43 Da and at 55 Da respectively and at 425 and 445 °C, the base peak was at 123 Da. Furthermore, peaks at m/z=60 Da [CH_2CH_2S], 87 Da [$CH_2CHCH_2CH_2S$], 116 Da [$CO(CH_2)_4S$, $CH_2CHCH_2CH_2SCHO$] and 135 Da [HSCHOCHOHCHOHCH] were again among the most intense peaks.

In Table 3.7 the most intense and characteristic peaks recorded in the mass spectra at 380, 400, 425 and 445° C and the assignments made are given.

Single ion evolution profiles of some selected products, namely OHCHCH (m/z=43 Da), $CH_2CH_2CHCH_2$ (m/z=55 Da), CHOHCHOH, CH_2CH_2S ((m/z=60 Da), $CH_2CHCH_2CH_2S$ (m/z=87 Da), (m/z=101 Da), $CH_2CHCH_2CH_2SCH_2$ (m/z=110 Da), $CO(CH_2)_4S$, $CH_2CHCH_2CH_2SCHO$ (m/z=116 Da), $HSCHOCHOHCH_2OH$ (m/z=123 Da), HSCHOCHOHCHOHCH (m/z=135 Da), $CH_2NCO(CH_2)_4SCHCH_2$ (m/z=171 Da), $H(HCOH)_4OCHSH$ (m/z=183 Da), $CF_3(CF_2)_5(CH_2)_2SCH_2$ (m/z=393 Da) and $CF_3(CF_2)_5(CH_2)_2S{=}CH_2CH_2CH_2CH_2CO$ (m/z=463 Da) are shown in Figure 3.12.

Characteristic peaks due to PBOX-Perf were quite significant although the sample modified with only one percent of the mercaptan used in the modification of PBOX-Perf.

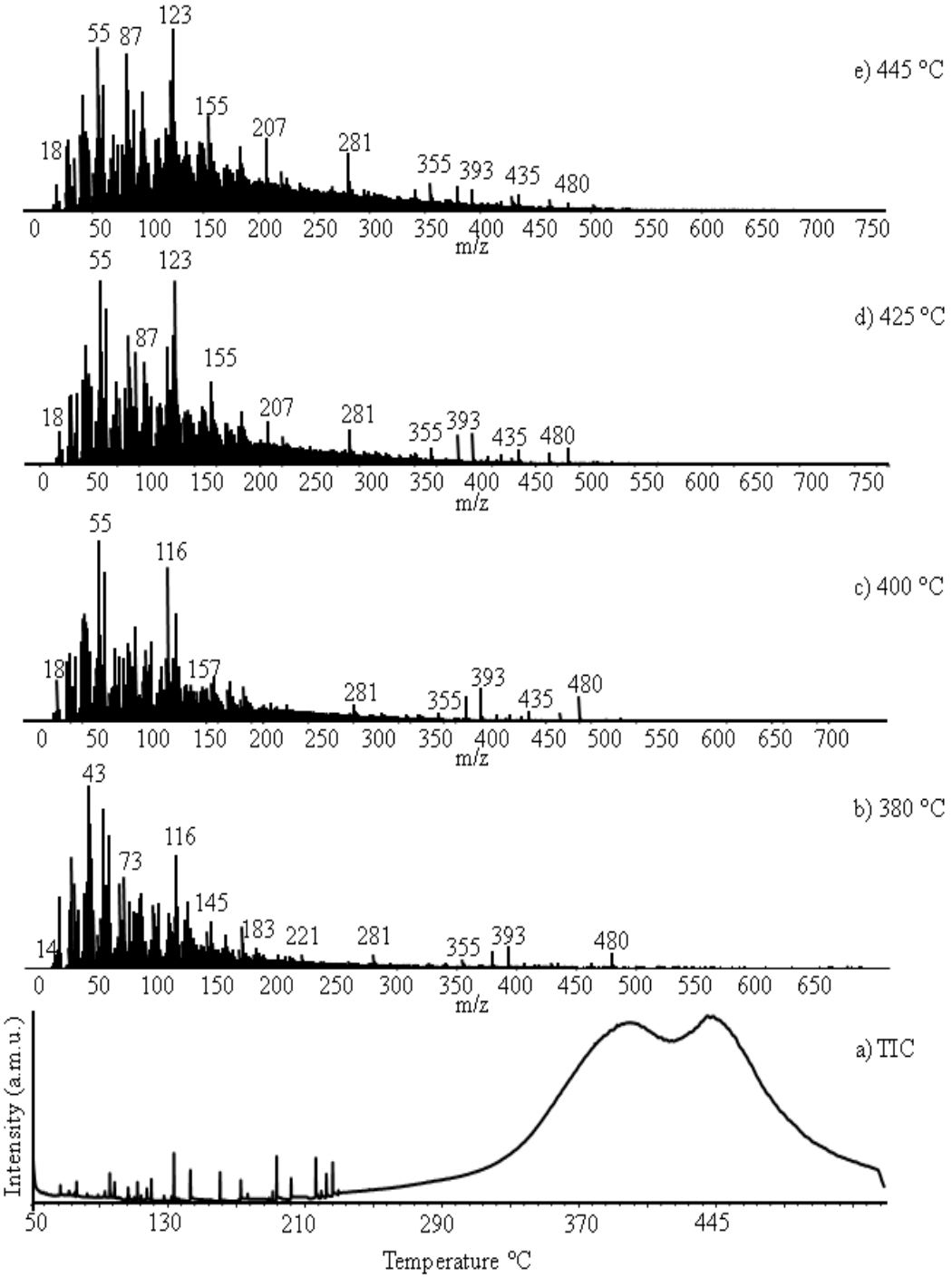

Figure 3.11: Pyrolysis mass data for PBOX-SP1.

Table 3.7: The relative intensities (RI) detected during the PBOX-SP1 pyrolysis and chemical assignments of the most intense and characteristic peaks in the mass spectrum of PBOX-SP1 380, 400, 425 and 445° C.

m/z	RI				Assignment
	380°C	400°C	425°C	445°C	
43	1000	600	366	348	OHCHCH
55	869	1000	997	898	$CH_2CH_2CHCH_2$
60	726	823	849	688	CHOHCHOH, CH_2CH_2S
87	404	526	609	553	$CH_2CHCH_2CH_2S$
98	299	273	279	301	$C_2H_4NCOC_2H_4$,$NCO(CH_2)_4$, $CH_2NCOC_3H_6$
101	349	443	371	228	$CH_2CHCH_2CH_2SCH_2$
110	297	301	305	366	$CH_2CH_2NCOCH_2CHCH$
116	616	849	637	450	$CO(CH_2)_4S$, $CH_2CHCH_2CH_2SCHO$
123	257	598	1000	1000	$HSCHOCHOHCH_2OH$
135	99	167	300	384	HSCHOCHOHCHOHCH
142	197	165	167	204	$CH_2NCOCHCHCH_2CH_2S$
171	225	217	223	254	$CH_2NCO(CH_2)_4SCHCH_2$
172	134	140	183	225	$CH_2NCO(CH_2)_4SCH_2CH_2$
183	105	192	287	348	$H(HCOH)_4OCHSH$
281	71	92	194	317	$CF_3CFCF(CF_2)_3$, $(CH_2CH_2NCO)_3CH_2CH_2N{=}COH$, $(CH_2CH_2NCO)_3CH_2CH_2N{=}COH$
335	8	20	39	65	$SCH_2CH_2C_6F_8(OH)_3$
393	111	179	169	115	$CF_3(CF_2)_5(CH_2)_2SCH_2$
435	21	52	81	85	$CF_3(CF_2)_5CH_2CH_2SCH_2CH_2CH_2CH_2$
463	19	45	67	66	$CF_3(CF_2)_5(CH_2)_2SCH_2CH_2CH_2CH_2CO$
480	81	136	91	41	$HCO(CH_2)_4SCH_2CHOH(CF_2)_5CF_3$

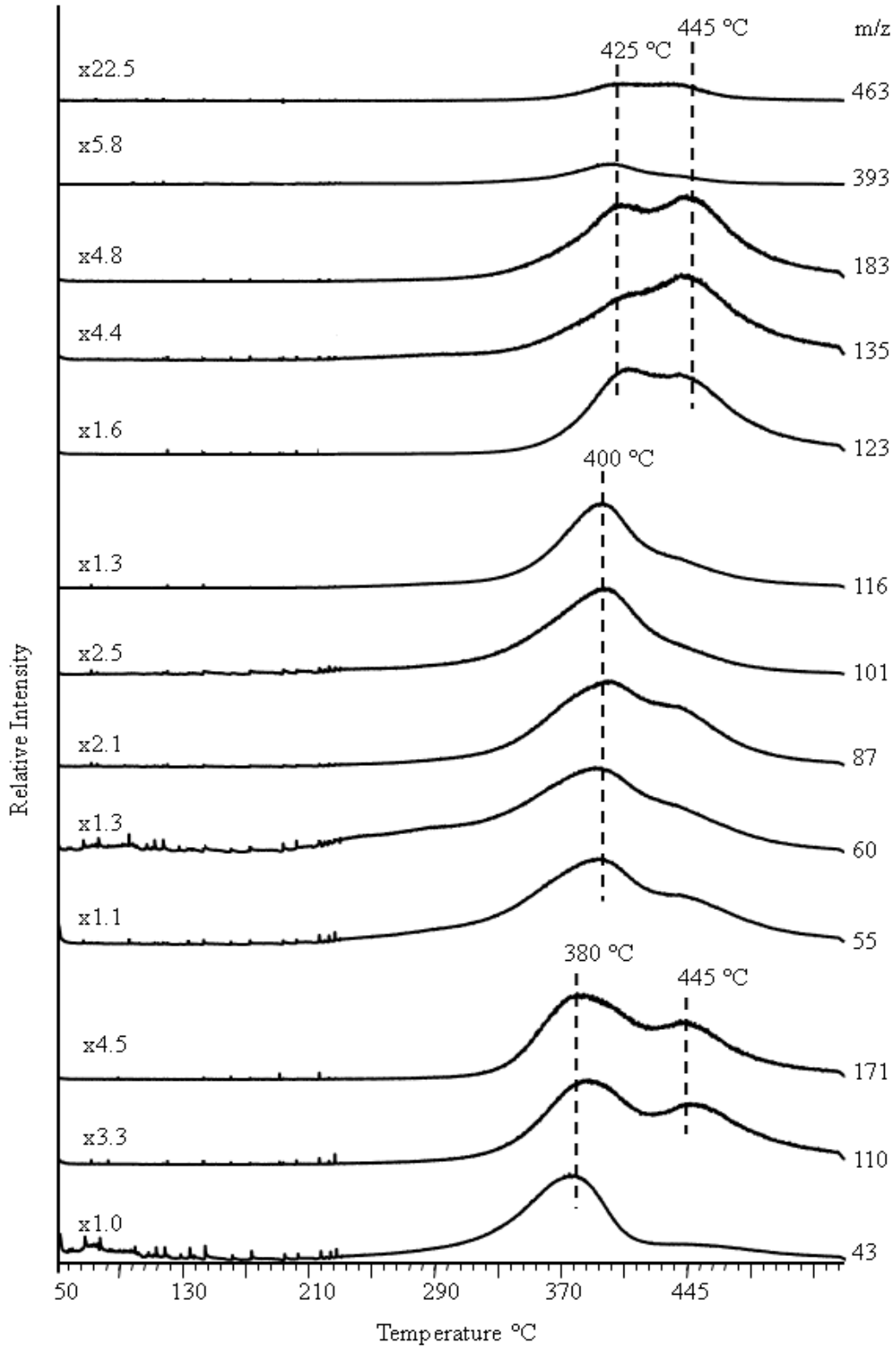

Figure 3.12: Single ion evolution pyrograms of some selected pyrolysis compounds obtained by direct pyrolysis of PBOX-SP1.

One point that should be noticed was the disappearance of the low temperature evolutions detected in case of PBOX-Perf. Another point that should also be noticed was the detection of significantly intense 55 Da peak that was associated with $CH_2CH_2CHCH_2$ fragment. Comparison of the trends in the evolution profiles of characteristics products of PBOX-Sug with the ones of PBOX-SP1 indicated an increase in thermal stability of thio-β-glucose unit significantly; the evolutions around 310 and 320 °C detected for PBOX-Sug totally disappeared for PBOX-SP1. Similarly low temperature evolutions detected during the pyrolysis of PBOX-Perf, in the temperature range between 300 and 350 °C also disappeared during the pyrolysis of PBOX-SP1. Single ion evolution profiles of degradation products showed maxima at different temperatures indicating presence of units with different thermal stabilities. However, variations in the position of peak maxima were noticeably smaller (380, 400, 425 and 445 °C) than those were observed for PBOX-Perf (67, 310, 332 and 445 °C) and PBOX-Sug (310, 320, 410 and 445 °C). It can be concluded that a thermally more homogeneous polymer was obtained by modification with 99% mercaptan of PBOX-Sug and 1% mercaptan of PBOX-Perf.

In Figure 3.13 single ion evolution profiles of some diagnostic products generated during pyrolysis of PBOX-Sug, PBOX-Perf and SP1 are shown for a better comparison. These products were mainly generated upon decomposition of the side chains generated by loss of glucose and perf units. Disappearance of low temperature evolutions pointed out stabilization of glucose units in the presence of 1H,1H,2H,2H-perfluoro-octanethiol.

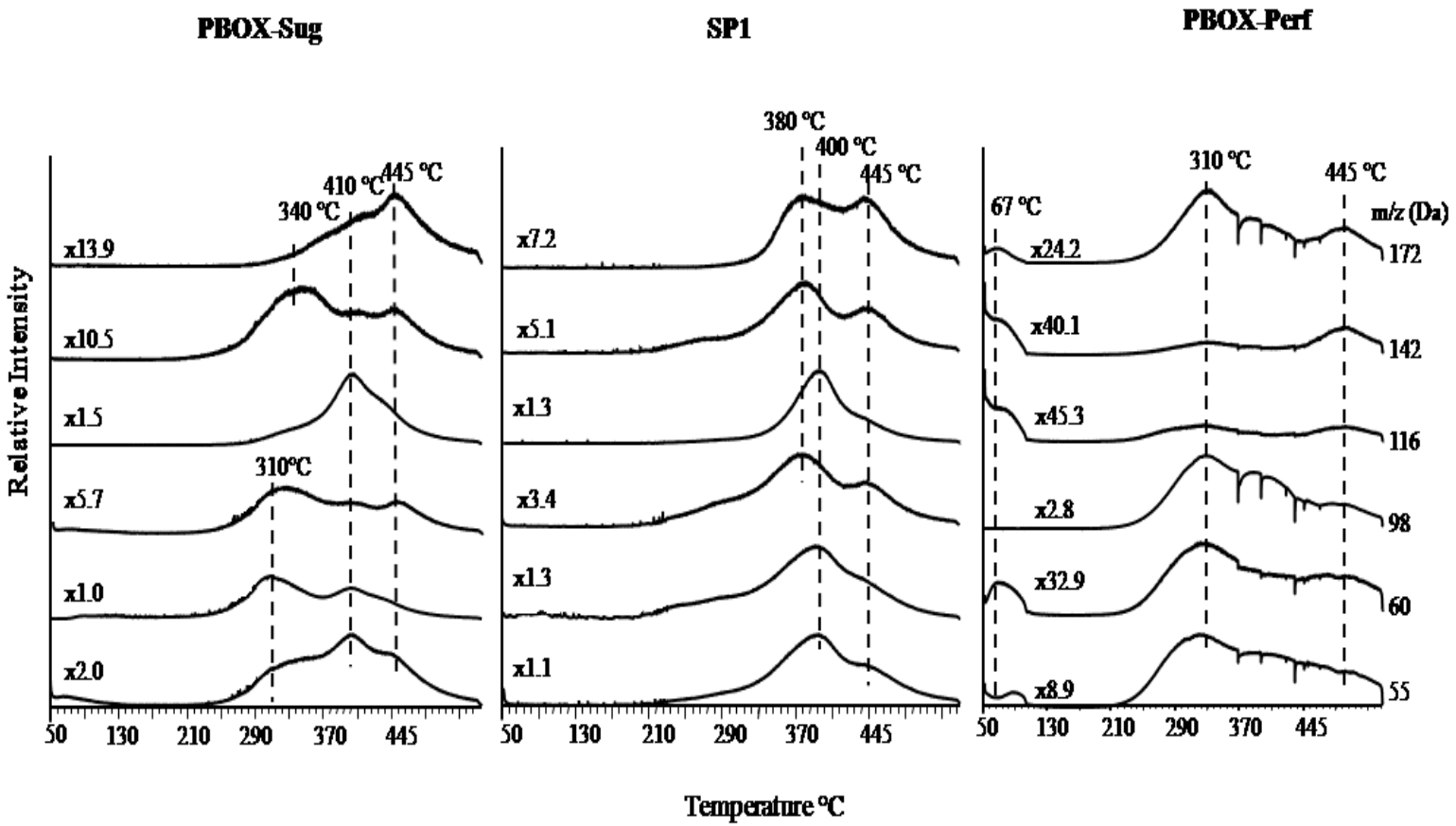

Figure 3.13: Single ion evolution profiles of some diagnostic products detected during the pyrolysis of PBOX-Sug, SP1 and PBOX-Perf

3.7 Poly(2-(3-butenyl)-2-oxazoline) modified with a mixture of 99% 3-mercapto-1,2 propanediol and 1% 1H,1H,2H,2H-perfluoro-octanethiol (PBOX-TP1).

The TIC curve of PBOX-TP1 is given in Figure 3.14. It showed a broad and weak peak with a maximum at around 210 °C, besides an intense peak with a maximum at around 425 °C (Figure 3.14). The base peak at 210 °C is at 28 Da, 240 °C is at 57 whereas, at 400, 425 and 445 °C, it is at 55 Da. In Table 3.8 the most intense and characteristic peaks recorded in the mass spectra at 210, 240, 400, 425 and 445 °C and their assignments made are given.

Contrary to what were observed for PBOX-Thiop and PBOX-Perf, no peak below 100 °C was detected in the TIC curve for this sample. However, the mass spectra recorded at around 210 °C were dominated with peaks that were present in the mass spectra of PBOX-Perf recorded below 100 °C (Figure 3.14). Presence of these peaks indicated evolution of $(CF_3(CF_2)_5(CH_2)_2S)_2$. The high mass peaks that can readily be associated with parent ion (m/z=758 Da) and fragment ions $CF_3(CF_2)_5(CH_2)_2SH$ (m/z=380 Da), $CF_3(CF_2)_5(CH_2)_2S\text{-}S$ (m/z=411 Da) and $CF_3(CF_2)_5(CH_2)_2SSCH_2$ (m/z=425 Da) were quite significant in this region.

The base peak in the low temperature mass spectra of PBOX-Thiop at 205 Da was now quite weak. The base peak was now at 28 Da due to C_2H_4 and/or CO. Other intense peaks were at 57 (CFC_2H_2, C_4H_9), 69 (CF_3), 77 ($CF_2CH{=}CH_2$, SCH_2CH_2OH) and 89 Da ($CH_2SCHCHOH$). The 57 Da peak may be attributed to C_3H_2F, C_4H_9 and/or C_2H_5O. The 69 Da peak can readily be attributed to CF_3 fragment. Products such as C_3H_2F and $C_4H_3F_2$ that may be generated by loss of F atoms may give rise to peaks at 77 and 89 Da.

$(CF_3(CF_2)_5(CH_2)_2S)_2$ peak totally disappeared in the pyrolysis mass spectra recorded at elevated temperature. The base peak was at 55 Da in this region as in the case of PBOX-Thiop. Other characteristic peaks of PBOX-Thiop such as 101 ($CH_2CHCH_2CH_2SCH_2$), 116 ($CO(CH_2)_4S$), 123 ($CH_2CHNCOCHCH_2CHCH_2$), 132

(CF_2CF_2CHF) and 157 Da ($CH_2CHNCO(CH_2)_4S$, $C_2H_4NCO(CH_2)_3CH=S$) were also present in the spectra. However their relative intensities changed significantly (Figure 3.15).

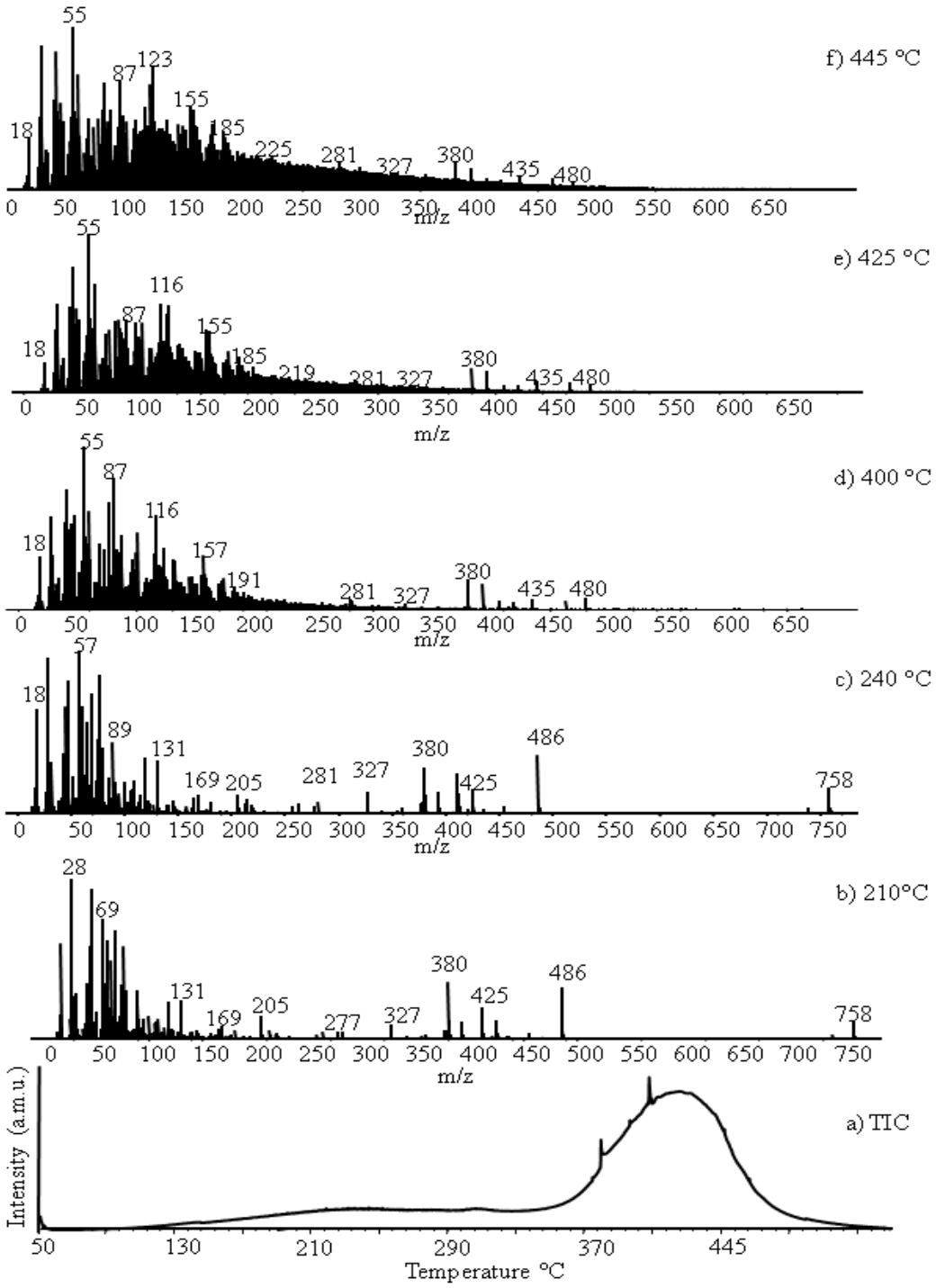

Figure 3.14: Pyrolysis mass data for PBOX-TP1

Table 3.8: The relative intensities (RI) detected during the PBOX-TP1 pyrolysis and chemical assignments of the most intense and characteristic peaks in the mass spectrum of PBOX-TP1 at 210, 240, 400, 425 and 445 °C.

m/z	RI					Assignment
	210°C	240°C	400°C	425°C	445°C	
28	1000	953	605	556	731	C_2H_4 , CO
45	603	660	561	534	549	CH_2CH_2OH , $CFCH_2$
47	935	814	615	459	427	CH_2SH
55	73	96	1000	1000	1000	$CH_2CH_2CHCH_2$
57	841	1000	480	369	376	CFC_2H_2, C_4H_9
69	665	739	432	371	400	CF_3
77	578	852	704	450	414	$CF_2CH{=}CH_2$, SCH_2CH_2OH
81	63	75	860	459	479	CF_2CF
89	355	438	138	146	179	$CH_2SCHCHOH$
91	154	191	146	174	140	$CFCH_2CH_2S$, $CH_2SCH_2CH_2OH$
101	28	50	506	446	433	$CH_2CHCH_2CH_2SCH_2$
107	117	149	181	283	354	$CH_2OHCHOHCH_2S$
109	157	203	206	276	381	$SCHCH_2CF_2$
116	10	16	616	560	534	$CO(CH_2)_4S$
119	265	340	288	325	377	CF_3CF_2, $CFCH_2CH_2SCH_2CH_2$
121	42	57	285	498	647	$CH_2SCH_2CHOHCH_2OH$
123	48	66	407	551	718	$CH_2CHNCOCHCH_2CHCH_2$
131	270	323	328	295	339	CF_2CFCF_2
132	16	27	320	310	332	CF_2CF_2CHF
147	32	50	217	256	301	$(CH_2)_4SCH_2CHOHCH_3$
155	7	6	224	396	527	$CH_2SCH_2CH_2CFCF_2$
157	19	25	358	393	463	$CH_2CHNCO(CH_2)_4S$, $C_2H_4NCO(CH_2)_3CH{=}S$
163	28	34	126	182	258	$(CF_2)_3CH$
169	97	117	165	191	245	$CF_3(CF_2)_2$, $CH_2CH_2S(CH_2)_2CF{=}CF_2$
181	56	68	125	173	215	$C_2H_4SC_2H_4C_3F_3$, $C_3H_5SC_2H_3CFCF_2$
205	137	118	60	95	154	$CF_2{=}CFCF_2CH_2CH_2SCH_2$
214	45	91	46	87	147	$CH_2CH_2CH_2SCH_2CH_2CFCFCF_2$
327	106	132	36	50	83	$CF_3(CF_2)_4CFCHCH_2$
359	32	37	11	26	57	$CF_3(CF_2)_4CFCHCH_2S$
380	387	282	194	153	158	$CF_3(CF_2)_5(CH_2)_2SH$
393	116	133	167	141	129	$C_6F_{12}HC_2H_4S_2$, $C_6F_{12}C_2H_4S_2H$,$C_6F_{13}C_2H_4SCH_2$
407	8	9	58	49	56	$CF_3(CF_2)_5(CH_2)_2SCH_2CH_2$
411	230	250	7	15	33	$CF_3(CF_2)_5(CH_2)_2SS$
419	3	5	50	50	56	$CF_3(CF_2)_5(CH_2)_2SCH_2CHCH$
425	141	148	4	12	28	$CF_3(CF_2)_5(CH_2)_2SSCH_2$
435	15	27	66	69	81	$CF_3(CF_2)_5(CH_2)_2SCH_2CH_2CH_2CH_2$
455	38	43	3	8	18	$CF_3(CF_2)_3(CHF)_2(CH_2)_2S(CH_2)_4CONCH_2$
463	5	6	61	63	64	$CF_3(CF_2)_5(CH_2)_2S{=}CH_2CH_2CH_2CH_2CO$
758	137	156	0	0	0	$(CF_3(CF_2)_5(CH_2)_2S)_2$

Single ion evolution of some selected products, namely C_2H_4, CO (m/z=28 Da), CH_2CH_2OH, $CFCH_2$ (m/z=45 Da), CH_2SH (m/z=47 Da), $CH_2CH_2CHCH_2$ (m/z=55 Da), CFC_2H_2, C_4H_9 (m/z=57 Da), CF_3 (m/z=69 Da), $CF_2CH=CH_2$, SCH_2CH_2OH (m/z=77 Da), $CH_2SCHCHOH$ (m/z=89 Da), $CH_2CHCH_2CH_2SCH_2$ (m/z=101 Da), $SCHCH_2CF_2$ (m/z=109 Da), $CO(CH_2)_4S$ (m/z=116 Da), [$CH_2CHNCOCHCH_2$ $CHCH_2$] (m/z=123 Da), CF_2CF_2CHF (m/z=132 Da), $CH_2CHNCO(CH_2)_4S$, $CH_2CH_2NCO(CH_2)_3CH=S$ (m/z=157 Da), $CH_2CH_2SCH_2CH_2CFCFCF$, CH_2CHCH_2 $SCH_2CHCFCF_2$ (m/z=181 Da), $CF_2=CFCF_2CH_2CH_2SCH_2$ (m/z=205 Da), $CH_2CH_2CH_2SCH_2CH_2CFCFCF_2$ (m/z=214 Da), $CF_3(CF_2)_4CFCHCH_2$ (m/z=327 Da), $CF_3(CF_2)_5(CH_2)_2SH$ (m/z=380 Da), $CF_3(CF_2)_5(CH_2)_2SS$ (m/z=411 Da), $CF_3(CF_2)_5(CH_2)_2SCH_2CHCH$ (m/z=419 Da) and [$CF_3(CF_2)_3(CHF)_2(CH_2)_2S$ $(CH_2)_4CONCH_2$] (m/z=455 Da) are shown in Figure 3.15.

Evolution profiles of some diagnostic products detected during the pyrolysis of PBOX-Thiop, PBOX-Perf and TP1 are given in Figure 3.16.

Unlike SP1, $(CF_3(CF_2)_5(CH_2)_2S)_2$ dimer was detected for this sample as in case of PBOX-Perf. However, its evolution shifted to higher temperatures. Again a thermally homogeneous polymer was produced in the presence of 1% mercaptan (1H,1H,2H,2H-perfluoro-octanethiol). Actually PBOX-Thiop was the thermally most stable among the modified PBOX polymers.

The high temperature evolutions detected for PBOX-Thiop and PBOX-Perf, was not recorded for TP1. It may be thought that for PBOX-Thiop and PBOX-Perf when the end groups of side chains were lost at low temperatures, coupling of these radicals took place generating units with relatively high thermal stability. It may further be thought that in the presence of 1% mercaptan used in the modification of PBOX-Perf, these coupling processes were inhibited and decomposition of side chains and polymer backbone occurred almost in the same temperature range.

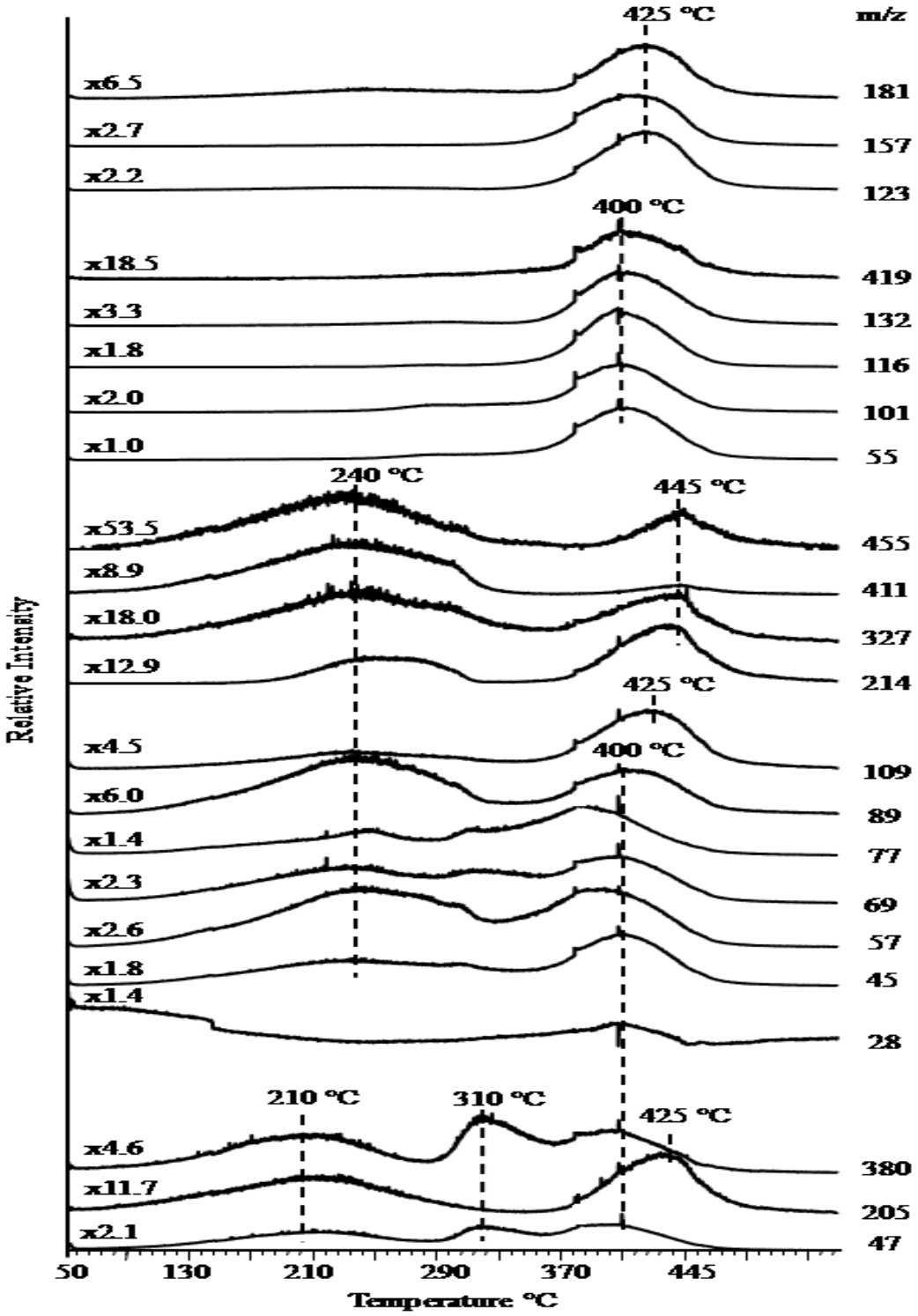

Figure 3.15: Single ion evolution pyrograms of some selected pyrolysis compounds obtained by direct pyrolysis of PBOX-TP1.

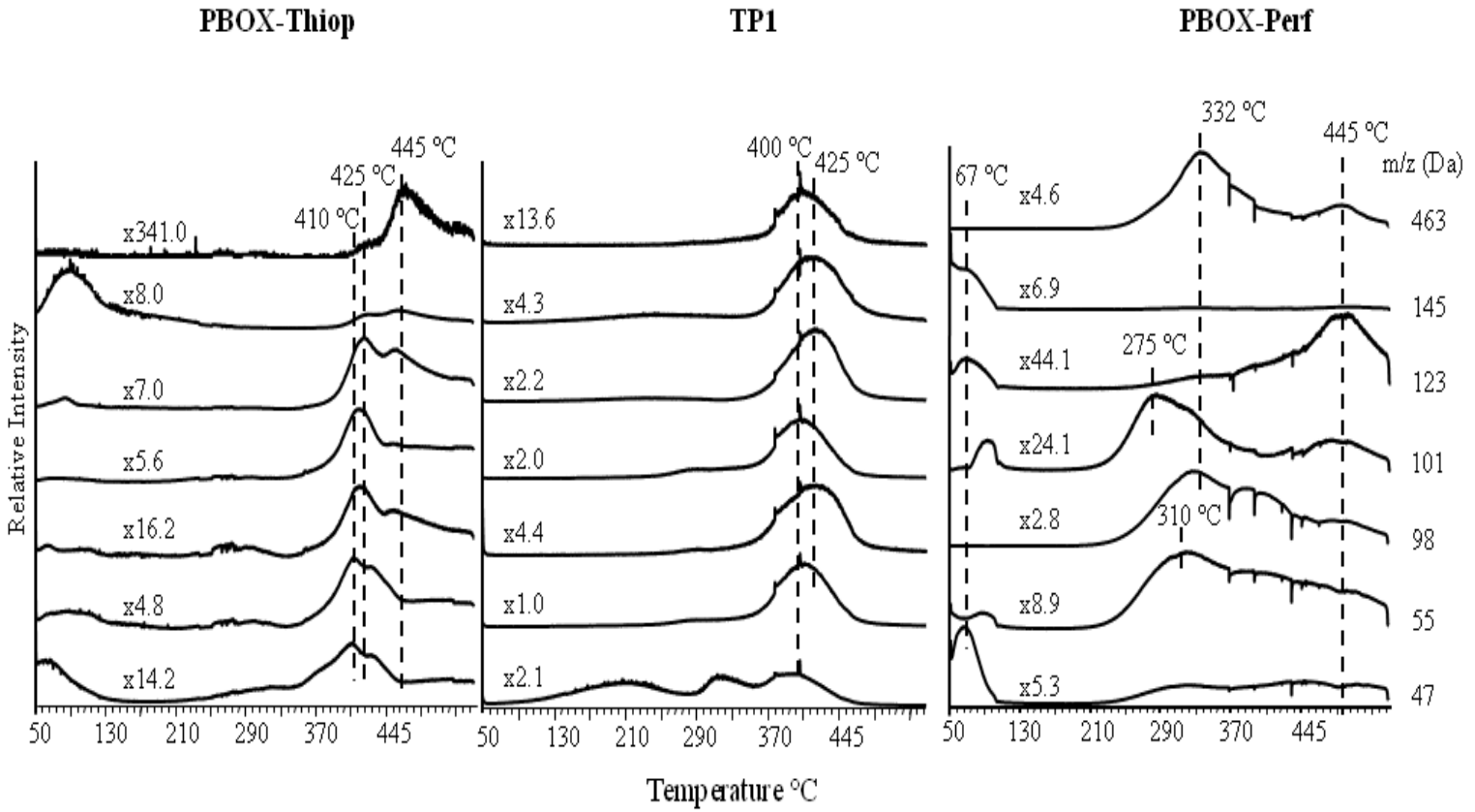

Figure 3.16: Single ion evolution profiles of some diagnostic products detected during the pyrolysis of PBOX-Thiop, TP1 and PBOX-Perf

CHAPTER 4

CONCLUSIONS

In this study, the thermal characteristics of poly(2-isopropyl-2-oxazoline) (PIPOX), poly(2-(3-butenyl)-2-oxazoline) (PBOX) and modified PBOX polymers such as PBOX-Perf, PBOX-Thiop, PBOX-Sug, PBOX-SP and PBOX-TP modified with 1H,1H,2H,2H- perfluoro-octanethiol, 3-mercapto-1,2 propanediol, thio-β-D-glucose derivative, mixture of thio-β-D-glucose derivative and 1H,1H,2H,2H-perfluoro-octanethiol and mixture of 3-mercapto-1,2 propanediol and 1H,1H,2H,2H-perfluoro-octanethiol respectively were investigated by direct pyrolysis mass spectrometry technique.

The results of this study can be summarized as;

PIPOX is the thermally most stable and homogeneous polymer among the polymers under investigation. Thermal degradation of PIPOX yielded mainly protonated monomer and oligomers. Thermal stability decreased when isopropyl side chains were replaced by butenyl groups indicating that presence of isopropyl side chains enhances thermal stability. For the polymer in which isopropyl groups were replaced by butenyl groups, namely, PBOX, the yield of protonated monomer and oligomers decreased noticeably. It may be thought that in the presence of the unsaturated butenyl groups, formation of oligomers, depolymerization reactions were inhibited most probably due to crosslinking of the groups generated during decomposition of side chains.

Almost similar thermal degradation behavior was observed for PIPOX50 and PIPOX90 where 50 and 90 indicate the number of repeating units. So it can be concluded that the number of repeating units in this range do not have any significant effect on the thermal behavior of PIPOX.

Modifications of PBOX with different mercaptans namely with 3-mercapto-1,2 propanediol (PBOX-Thiop), 1H,1H,2H,2H-perfluoro-octanethiol (PBOX-Perf) and thio-β-D-glucose derivative (PBOX-Sug) affected both thermal stability and thermal degradation products. For PBOX-Thiop and PBOX-Perf, presence of unreacted mercaptan and its dimer was confirmed by detection of low temperature evolutions. However, low temperature evolutions were not observed for PBOX-Sug, PBOX-SP1 and PBOX-TP1. Thermal degradation of modified samples was started by decomposition of side chains. The decomposition of the polymer backbone chains occurred at relatively high temperatures compared to side chains. Among the modified samples, PBOX-Thiop is thermally most stable. The temperature region where thermal degradation of side chains occurred shifted from 300 to 410 °C by modification of PBOX with 3-mercapto-1,2 propanediol. However a significant decrease in the thermal stability was observed when PBOX was modified with 1H, 1H,2H,2H-perfluoro-octanethiol. For PBOX-Sug obtained from modification of PBOX with thio-β-D-glucose derivative, change in thermal stability was not significant compared to PBOX-Perf.

Evolution of monomer was detected for PIPOX, PBOX, PBOX-Perf and PBOX-Thiop. However, monomer peak was not recorded for PBOX-Sug. This behavior may be attributed to presence of relatively unstable glucose unit.

Thermally more homogeneous polymers were obtained when PBOX was modified with a mixture of two mercaptans (PBOX-SP1, PBOX-TP1). Although the percentage of mercaptan 1H,1H,2H,2H-perfluoro-octanethiol used in the preparation of PBOX-TP1 and PBOX-SP1 was only 1%, a significant effect on thermal behavior was noted. Thermal stability of the glucose units were increased drastically in case

of PBOX-SP1. On the other hand, although thermally more homogeneous sample was obtained due to the increase in thermal stability of side chains, a slight decrease in the thermal stability of the main chain was observed for PBOX-Thiop in the presence of 1% mercaptan 3-mercapto-1,2 propanediol. It may be concluded that in the presence of 1H,1H,2H,2H-perfluoro-octanethiol, strong interactions between hydroxides of glucose units and octanethiol took place. This inturn increased the thermal stability of both glucose and octanethiol units. However, when the thermal stability of thionyl groups increased, the coupling of end groups generating relatively more stable polymer backbone for PBOX-TP1 was limited compared to PBOX-Thiop.

REFERENCES

1- Kumar A., Srivastava A., Galaev I., Mattiasson B., 'Smart polymers: Physical forms and bioengineering applications', *Progress in Polymer Science*, 2007, 32, p.1205-1237

2- Lambermont-Thijs H.M.L., Van Kuringen H.P.C., Van der Put J.P.W., Schubert U.S., Hoogenboom R., 'Temperature Induced Solubility Transitions of Various Poly(2-oxazoline)s in Ethanol-Water Solvent Mixtures', *Polymers,* 2010, 2, p.188-199

3- Meyer M., Antonietti M., Schlaad H., 'Unexpected Thermal Characteristics of Aqueous Solutions of Poly(2-isopropyl-2-oxazoline)', *Soft Matter,* 2007, 3, p.430-431 (and references therein)

4- Kutz M., Handbook of Materials Selection, 2002, p. 412

5- De las Heras Alarco´n C., Pennadam S., Alexander C., 'Stimuli responsive polymers for biomedical applications', *Chem. Soc. Rev*., 2005, 34, p.276–285

6- Park J.S., Kataoka K., 'Comprehensive and Accurate Control of Thermosensitivity of Poly(2-alkyl-2-oxazoline)s via Well-Defined Gradient or Random Copolymerization', *Macromolecules,* 2007, 40, p.3599-3609

7- Heskins M., James E., Guillet J., 'Solution properties of poly(N-isopropylacrylamide)', *Macromol. Sci. Chem.,* 1968, 2(8), p.1441-1455.

8- Demirel A. L., Meyer M., Schlaad H., 'Formation of Polyamide Nanofibers by Directional Crystallization in Aqueos Solution', *Angew. Chem. Int. Ed*., 2007, 46, p.8622-8624

9- Gress A., Smarsly B., Schlaad H., 'Formation of Glycopolyamide Nanofibers', *Macromolecular Rapid Communications*, 2008, 29, p.304-308

10- Huber S., Hutter N., Jordan R., 'Effect of end group polarity upon the lower critical solution temperature of poly(2-isopropyl-2-oxazoline)', *Colloid Polym Sci.*, 2008, 286, p.1653–166

11- Weber C., Becer R., Hoogenboom R., Schubert U. S., 'Lower Critical Solution Temperature Behavior of Comb and Graft Shaped Poly[oligo(2-ethyl-2-oxazoline)methacrylate]s', *Macromolecules*, 2009, 42, p.2965-2971

12- Hoogenboom R., Thijs H.M.L., Jochems M.J.C.H., Lankvelt B.M.V., Fijten M.W.M., Schubert U.S., 'Tuning the LCST of poly(2-oxazoline)s by varying composition and molecular weight: alternatives to poly(N-isopropylacrylamide)', *Chem. Commun.,* 2008, p.5758–5760

13- Schlaad H., Diehl C., Gress A., Meyer M., Demirel A.L., Nur Y., Bertin A., 'Poly(2-oxazoline)s as Smart Bioinspired Polymers', *Macromol. Rapid Commun.*, 2010, p.511-525 (references therein)

14- Diehl C., Schlaad H., 'Thermo-Responsive Polyoxazolines with Widely Tuneable LCST', *Macromol. Biosci.,* 2009, 9, p.157–161

15- Aoi K., Suzuki H., Okada M., 'Architectural control of sugar-containing polymers by living polymerization: ring-opening polymerization of 2-oxazolines initiated with carbohydrate derivatives', *Macromolecules*, 1992, 25 (25), p.7073–7075

16- Hoogenboom R., Fıjten M.W.M., Schubert U.S., 'Parallel Kinetic Investigation of 2-Oxazoline Polymerizations with Different Initiators as Basis for Designed Copolymer Synthesis', *Journal of Polymer Science: Part A: Polymer Chemistry*, 2004, Vol. 42, p.1830–1840 (and references therein)

17- Hoogenboom R., 'Poly(2-oxazoline)s: A polymer class with numerous potential applications', *Angew Chem Int Ed Engl.* 2009, 48(43), p.7978-94.

18- Adams N., Schubert U.S., 'Poly(2-oxazolines) in Biological and Biomedical Application Contexts', *Advanced Drug Delivery Reviews,* 2007, 59(15), p.1504-20.

19- Hoogenboom R., Fıjten M.W.M., Thijs H.M.L., Lankvelt B.M., Schubert U.S., 'Microwave-assisted synthesis and properties of a series of poly(2-alkyl-2-oxazolines)s', *Designed Monomers and Polymers,* 2005, Vol. 8, No. 6, p. 659–671

20- Wiesbrock F., Hoogenboom R., Abeln C. H., Schubert U.S., 'Single-Mode Microwave Ovens as New Reaction Devices: Accelerating the Living Polymerization of 2-Ethyl-2-Oxazoline', *Macromol. Rapid Commun.,* 2004, 25, p.1895–1899

21- Huber S., Jordan R., 'Modulation of the lower critical solution temperature of 2-Alkyl-2-oxazoline copolymers', *Colloid Polym Sci.*, 2008, 286, p.395–402

22- Haruna, M.,'Synthesis and Characterization of Temperature Responsive poly(2-ethyl-2-oxazoline)', *Bayero Journal of Pure and Applied Sciences,* 2010, 3(1), p.250 – 254

23- Morimoto N., Obeid R., Yamane S., Françoise M.W., Akiyoshi K., 'Composite nanomaterials by self-assembly and controlled crystallization of poly(2-isopropyl-2-oxazoline)-grafted polysaccharides', *Soft Matter*, 2009, 5, p.1597–1600

24- Thijs H.M.L., Hoogenboom R.,Fustin C.A., D'Haese C.B., Gohy J.F., Schubert U.S., 'Solubility Behavior of Amphiphilic Block and Random Copolymers Based on 2-Ethyl-2-oxazoline and 2-Nonyl-2 oxazoline in Binary Water–Ethanol Mixtures', *Journal of Polymer Science: Part A: Polymer Chemistry*, 2009, Vol. 47, p.515–522

25- Kempe K., Lobert M., Hoogenboom R., Schubert U.S., 'Synthesis and Characterization of a Series of Diverse Poly(2-oxazoline)s', *Journal of Polymer Science: Part A: Polymer Chemistry*, 2009, Vol. 47, p.3829–3838

26- Fustin C.A., Huang H., Hoogenboom R., Wiesbrock F., Jonas A.M., Schubert U.S., Gohy J.F., 'Evaporation induced micellization of poly(2-oxazoline) multiblock copolymers on surfaces', *Soft Matter*, 2007, 3, p.79–82

27- Kempe K., Vollrath A., Schaefer H.W. , Poehlmann T. G. , Biskup C., Hoogenboom R., Hornig S., Schubert U.S., 'Multifunctional Poly(2-oxazoline) Nanoparticles for Biological Applications', *Macromolecular Rapid Communications,* 2010, Vol. 31, p.1869-1873

28- Zhao J., Hoogenboom R., Assche G. V., Mele B.V., 'Demixing and Remixing Kinetics of Poly(2-isopropyl-2-oxazoline) (PIPOZ) Aqueous Solutions Studied by Modulated Temperature Differential Scanning Calorimetry', *Macromolecules*, 2010, 43, p.6853–6860

29- Park J-S., Kataoka K., 'Precise Control of Lower Critical Solution Temperature of Thermosensitive Poly(2-isopropyl-2-oxazoline) via Gradient Copolymerization with 2-Ethyl-2-oxazoline as a Hydrophilic Comonomer', *Macromolecules*, 2006, 39, p.6622-6630

30- Aguilar M.R., Elvira C., Gallardo A., Vázquez B., Román J.S., 'Smart Polymers and Their Applications as Biomaterials', *Topics in Tissue Engineering*, 2007, Vol. 3, Chapter 6

31- Kempe K., Lobert M., Hoogenboom R., Schubert U.S., 'Screening the Synthesis of 2-Substituted-2-oxazolines', *J. Comb. Chem*., 2009, 11, p.274–280

32- Caponi P.F., Qiu X.P., Vilela F., Winnik F.M., Ulijn R.V., 'Phosphatase/temperature responsive poly(2-isopropyl-2-oxazoline)', *Polymer Chemistry*, 2011, 2, p.306-308

33- Park J.S., Akiyama Y., Winnik F.M., Kataoka K., 'Versatile Synthesis of End-Functionalized Thermosensitive Poly(2-isopropyl-2-oxazolines)', *Macromolecules,* 2004, 37, p. 6786-6792

34- Obeid R., Park J.Y., Advincula R.C., Winnik F.M., 'Temperature-dependent interfacial properties of hydrophobically end-modified poly(2-isopropyl-2-oxazoline)s assemblies at the air/water interface and on solid substrates', *Journal of Colloid and Interface Science,* 2009, Volume 340, p. 142-152

35- Kranenburg J.M., Tweedie C.A., Hoogenboom R., Wiesbrock F., Thijs H.M.L., Hendriks C.E., Vliet K.J.V., Schubert U.S., 'Micro moduli for a diblock copoly(2-oxazoline) library obtained by highthroughput screening', *J. Mater. Chem*., 2007, 17, p.2713–2721

36- Diehl C., Černoch P., Zenke I., Runge H., Pitschke R., Hartmann J., Tiersch B., and Schlaad H., 'Mechanistic study of the phase separation/crystallization process of poly(2-isopropyl-2-oxazoline) in hot water', *Soft Matter*, 2010, 6, p.3784-3788

37- Gress A., Völkel A., Schlaad H., 'Thio-Click Modification of Poly(2-(3-butenyl)-2-oxazoline)', *Macromolecules,* 2007, 40 (22), p.7928-7933

38- Justynska J., Hordyjewicz Z., Schlaad H., 'New Functional Diblock Copolymers Through Radical Addition of Mercaptans', *Macromol. Symp.,* 2006, 240, p.41-46

39- You L., Schlaad H., 'An Easy Way to Sugar-Containing Polymer Vesicles or Glycosomes', *J. Am. Chem. Soc*., 2006, 128 (41), p. 13336-13337

40- Gruendling T., Weidner S., Falkenhagen J., Barner-Kowollik C., 'Mass spectrometry in polymer chemistry: a state-of-the-art up-date', *Polym. Chem.*, 2010, 1, p. 599-617

41- Gross M.L., Caprioli R.M., editor, 'Pyrolysis Mass Spectrometry for Molecular Ionization Methods', *The Encyclopedia of Mass Spectrometry*, 2007, Vol.6, p. 925-938

42- Nur Y., Çolak D.E., Chianga I., Yağcı Y., Hacaloğlu J., 'Pyrolysis of Poly(phenylene vinylene)s with PCL side chains', *Polymer Degradation and Stability*, 2008, 93, p.904-909